Applied Thermal Engineering 194 (2021) 117048

Contents lists available at ScienceDirect

Applied Thermal Engineering

journal homepage: www.elsevier.com/locate/apthermeng

# Calcium looping for power generation with $CO_2$ capture: The potential of sorbent storage for improved economic performance and flexibility

Marco Astolfi [a], Edoardo De Lena [a], Francesco Casella [b], Matteo Carmelo Romano [a,*]

[a] Politecnico di Milano, Department of Energy, via Lambruschini 4, 20156, Milano, Italy
[b] Politecnico di Milano, Department of Electronics, Information and Bioengineering, Via Ponzio 34/35, 20133 Milano, Italy

A R T I C L E I N F O

*Keywords:*
Calcium looping
Carbon capture
CCS
Part-load
Flexibility
Power plant

A B S T R A C T

The aim of this work is to investigate the potential of calcium looping (CaL) $CO_2$ capture system for power plants with sorbent storage, for flexible and low-emission power generation from coal. Two different CaL systems have been analyzed for $CO_2$ capture from a reference pulverized coal power plant: (i) a *Baseline* CaL system and (ii) a *FlexiCaL* system with sorbent storage. The sorbent storage systems can be exploited in two ways: the primary storage system allows to decouple the carbonator and the calciner load and reduce the size of the calciner island; the secondary storage unit allows to increase/reduce the maximum/minimum power output of the plant for improved grid services. Heat and mass balances have been computed at different loads with process simulation software, considering the off-design operation of the main plant components. A simplified economic analysis has been carried out to compute the cost of electricity and estimate the economic benefits of the primary sorbent storage system for a given power generation profile. The method used in this work allowed to compute the off-design behaviour of the CaL power plant with the highest accuracy among the literature studies and to understand the potential of the secondary solids storage to provide grid services for the first time.

The part-load analysis provided insights on the design of the carbonator reactor, that should limit the heat transfer surface in the riser to avoid excessive reactor cooling at part-load. Conversely, reaction heat should preferably be extracted from the external heat exchangers, where the heat transfer rate can be controlled more easily. From the thermodynamic standpoint, the two CaL plants feature similar efficiency on weekly cycling basis. The secondary storage allows increased operativity of the *FlexiCaL* plant on the secondary market, thanks to +2% of maximum power and −13% of minimum power output. The primary storage system allows reducing the capital cost of the CaL system, leading to LCOE reduction by 4–5% compared to the *Baseline* case, in a wide range of carbon tax and plant availability.

## 1. Introduction

Coal combustion in power plants is responsible for over 70% of $CO_2$ emissions from power generation worldwide [1]. Massive grow of renewable energy sources will be indispensable for achieving significant reduction of $CO_2$ emissions in the next decades. According to the Sustainable Development Scenario, by 2040 more than 40% of the global electricity generation will be supplied by intermittent renewable energy sources [2]. In this context, fossil fuel power plants are required to operate flexibly, i.e. with significant load variations, frequent startup and shutdowns, following the power demand and providing grid services.

In advanced economies, coal-fired power plants are being decommissioned and in most European countries phase-out is expected in the next decade. Nevertheless, coal will likely continue holding a significant share of power generation in economies highly dependent on this energy source (e.g. in Eastern Europe) and with recently installed capacity (e.g. in Asia, where coal plants are 11-years-old on average with decades left to operate) [3]. In these countries, $CO_2$ capture and storage (CCS) will be one of the bullets to meet the $CO_2$ emission targets in the next 30 years. As highlighted in [4], most of the coal-fired power plants in 2040 will be based on supercritical and ultra-super critical (USC) steam cycles, characterized by high energy efficiency and flexibility, thanks to once-through steam generators that can provide quicker load changes compared to conventional subcritical drum-type boilers [5].

In the last two decades, increasing efforts have been devoted to

* Corresponding author.
*E-mail address:* matteo.romano@polimi.it (M.C. Romano).

https://doi.org/10.1016/j.applthermaleng.2021.117048
Received 24 February 2021; Received in revised form 14 April 2021; Accepted 27 April 2021
Available online 3 May 2021

**Nomenclature**

*Acronyms*

| | |
|---|---|
| ASU | Air separation unit |
| BOP | Balance of plant |
| CaL | Calcium looping |
| CaLPP | Calcium looping power plant |
| Capex | Capital expenditure |
| CCF | Carrying Charge Factor |
| CCS | Carbon capture and storage |
| CF | Capacity factor |
| CFB | Circulating fluidized bed |
| CPU | $CO_2$ purification unit |
| DES | Design |
| EHE | External heat exchangers |
| FD | Forced draft |
| FG | Flue gas |
| FGD | Flue gas desulfurizer |
| FWH | Feed water heater |
| HHV | Higher heating value |
| HP | High pressure |
| ID | Induced draft |
| IP | Intermediate pressure |
| KPI | Key performance indicator |
| LCOE | Levelized cost of electricity |
| LHV | Lower heating value |
| LP | Low pressure |
| LT | Low temperature |
| MIN | Minimum |
| MT | Medium temperature |
| Opex | Operating expenditure |
| PC | Pulverized coal |
| PCPP | Pulverized coal power plant |
| PL | Part-load |
| RES | Renewable energy source |
| RH | Reheating |
| SC | Steam cycle |
| SH | Superheating |
| SOC | State of charge |
| SPECCA | Specific primary energy consumption for $CO_2$ avoided |
| TASC | Total as-spent cost |
| TSA | Temperature swing adsorption |
| UA | Overall heat transfer coefficient*Area |
| USC | Ultra-super critical |
| WE | Weekend |

*Symbols*

| | |
|---|---|
| $F_0$ | Limestone make up [$kmol_{Ca}/s$] |
| $F_{Ca}$ | Sorbent circulation rate [$kmol_{Ca}/s$] |
| $F_{CO2}$ | $CO_2$ flow rate at carbonator inlet [$kmol_{CO2}/s$] |
| $\eta$ | Efficiency [%] |
| $\eta_{QHT}$ | High temperature heat to electricity efficiency (eq. (1)) [%] |
| $\dot{W}$ | Electric power [MW] |
| $\dot{Q}$ | Thermal power [MW] |

*Subscripts and superscripts*

| | |
|---|---|
| aux | auxiliaries |
| BFW | boiler feedwater |
| calc | calciner |
| carb | carbonator |
| cond | condenser |
| e | electric |
| QHT | high temperature heat |
| st | steam turbine |
| tot | total |

increasing the flexibility of coal-fired power plants. Some of these techniques are commonly used in industrial environments such as the “condensate throttling” [6] for primary frequency control and control of the extracted steam for the high-pressure heaters [7,8].

For the most mature $CO_2$ capture technologies, some process alternatives have been proposed to increase the flexibility of power plants with CCS and their economic competitiveness through energy storage techniques. The way energy storage systems can be exploited is twofold: (i) to partly shift the parasitic energy consumption of the $CO_2$ capture plant from high electricity price hours to low electricity price ones and (ii) to size part of the capital-intensive $CO_2$ capture equipment on the average load rather than on the peak capacity. For example, in solvent-based capture plants, solvent storage allows to decouple the consumption of heat for solvent regeneration from the $CO_2$ capture rate and to downsize the solvent stripper and the $CO_2$ compression unit on the average plant load [9–12]. In oxyfuel systems, oxygen storage allows to decouple the energy intensive production of $O_2$ from the plant load and to downsize the capital-intensive air separation unit (ASU) [5,13–16]. The storage of high temperature solids has also been proposed with the same scope to manage daily load variation [17]. In pre-combustion $CO_2$ capture systems, hydrogen/syngas storage has been proposed to decouple hydrogen/syngas production from electric power output [13,18,19].

Calcium Looping (CaL) is an emerging post-/oxy-combustion $CO_2$ capture technology particularly promising for retrofit of coal power plants, that has been successfully demonstrated at TRL6 [20–22]. In the recent years, different aspects of CaL have been experimentally analyzed, both at laboratory scale and in pilot plants (up to $MW_{th}$ scale), demonstrating the process at steady-state conditions [20,23–25] and the evolution of sorbent properties over time [26,27]. Furthermore, experimental studies have been recently conducted at the La Pereda pilot plant, to investigate the dynamic evolution of the $CO_2$ carrying capacity of the limestone [28] and the impact of the load changes on carbonator $CO_2$ capture efficiency [29]. Modelling studies have been also carried out to assess the potential of energy storage in CaL power plants. Criado et al. and Arias et al. assessed the possibility of storing large amounts of Ca-based sorbent at relatively low temperature to capture the $CO_2$ from back-up coal power plants (i.e. expected to operate with very low capacity factor, suitable for seasonal energy storage) [30,31]. This allows a significant capital cost saving deriving from the downsized calciner, $O_2$ production and $CO_2$ compression islands, that are operated at base load. Hanak et al. assessed the energy storage in CaL power plants through liquid oxygen storage and high temperature sorbent storage, designed for daily cycling [32]. The authors of this paper also assessed the economic potential of high temperature sorbent storage in CaL power plants, determining the criteria for the economic optimal sizing of the storage silo and of the calcination island, that should be sized based on the expected daily cycling [33].

The scope of this study is to assess the potential of a sorbent storage system in a CaL process from techno-economic perspective, by comparing the key performance indicators of a baseline CaL power plant and an advanced plant with storage. In this paper, the following novel aspects are assessed and discussed with respect to the existing literature:

- a detailed modelling of the CaL system with a preliminary design of the reactors, heat exchangers and machines has been carried out, to provide insights on the design criteria of the carbonator reactor and

to predict with proper accuracy the performance of the CaL plant at part-load and the resulting cost of electricity;
- the potential of an additional secondary sorbent storage unit to expand the maximum-minimum power range and improve the capacity of operating on the secondary electricity market has been explored.

## 2. Description of the assessed plants

The general process flowsheet of the plant analyzed in this work is shown in Fig. 1, which represents the case of an existing pulverized coal-fired power plant (PCPP) coupled with a CaL system with sorbent storage units. The existing PCPP is based on an air combustion boiler burning low sulfur bituminous coal (Table 1) and an Ultra Super Critical (USC) steam cycle already described in [33]. Table 2 reports the main results for the PCPP design (DES) and part-load (PL) operations, obtained by a progressive reduction of the combustion power. At part-load, the net power output is obtained as the difference between the gross steam cycle power output, calculated with a specific off design efficiency curve [33], and the consumption of the boiler auxiliaries and the FGD, assumed proportional to the fuel consumption.

The PCPP load considered in this work follows a typical profile of a modern coal fired power plant in Central Europe, characterized by two periods at nominal fuel consumption (6–14 and 18–22) every day from Monday to Friday and a fuel consumption equal to 40% of the design value in the remaining of the time. Table 3 reports the average capacity factor for the gross power output and for the flue gases mass flow rate with respect to the nominal value in working days, weekend days and whole week.

The study was conducted by analyzing two different cases: the case without storage, referred to as *Baseline* case, and the case implementing storage concept, referred to as *FlexiCaL* case.

In the following subsections, a brief description of the main features and operating constraints of the three main sections of the assessed system is provided, namely: (i) the CaL system, (ii) the storage system and (iii) the Calcium looping power plant (CaLPP).

### 2.1. CaL system

The CaL system has been simulated with the proprietary code GS [34] and adopting the carbonator model described in [35]. The $CO_2$ compression and purification unit (CPU) was designed with Aspen Plus and modelled as a single flash, self-refrigerated process suitable for pipeline transport based on the scheme proposed in [36]. On the contrary, the air separation unit (ASU) is calculated as a black box with assumptions taken from literature [37]. A concise description of the two main sections of the CaL system (carbonator and calciner lines) is provided in this work, while a more detailed description can be found in

**Table 1**
Coal composition (as received) and heating values. Ash molar composition: 2/3 $SiO_2$, 1/3 $Al_2O_3$.

| Chemical specie | Mass% |
|---|---|
| C | 66.52% |
| N | 1.56% |
| H | 3.78% |
| O | 5.46% |
| S | 0.52% |
| Ash | 14.15% |
| Moisture | 8.01% |
| Lower heating value (LHV), MJ/kg | 25.17 |
| Higher heating value (HHV), MJ/kg | 26.23 |

**Table 2**
Main data of the existing coal-fired power plant at the design operating condition (DES) and different part-loads with fuel input equal to 40% (PL40), 60% (PL60) and 80% (PL80) of the design value.

| PCPP | DES | PL80 | PL60 | PL40 |
|---|---|---|---|---|
| Steam cycle gross power output, MW | 771.7 | 612.9 | 452.8 | 290.4 |
| Auxiliary power consumption, MW | 18.7 | 14.9 | 11.2 | 7.5 |
| FGD power, MW | 3.3 | 2.7 | 2.0 | 1.3 |
| BOP power, MW | 2.5 | 2.0 | 1.5 | 1.0 |
| Net power output, MW | 747.2 | 593.3 | 438.1 | 280.6 |
| Relative net power output, compared to the design | 100% | 79% | 59% | 38% |
| Fuel input, $MW_{LHV}$ | 1676.5 | 1341.2 | 1005.9 | 670.6 |
| Net efficiency, $\%_{LHV}$ | 44.6% | 44.2% | 43.6% | 41.8% |
| Coal consumption, kg/s | 66.61 | 53.29 | 39.96 | 26.64 |
| Flue gases mass flow rate, kg/s | 743.8 | 595.0 | 446.3 | 297.5 |
| Emitted $CO_2$, kg/s | 162.5 | 130.0 | 97.5 | 65.0 |
| $CO_2$ concentration, %vol. | 14.9% | 14.9% | 14.9% | 14.9% |
| Specific $CO_2$ emission, kg/MWh | 782.7 | 788.6 | 801.0 | 833.7 |

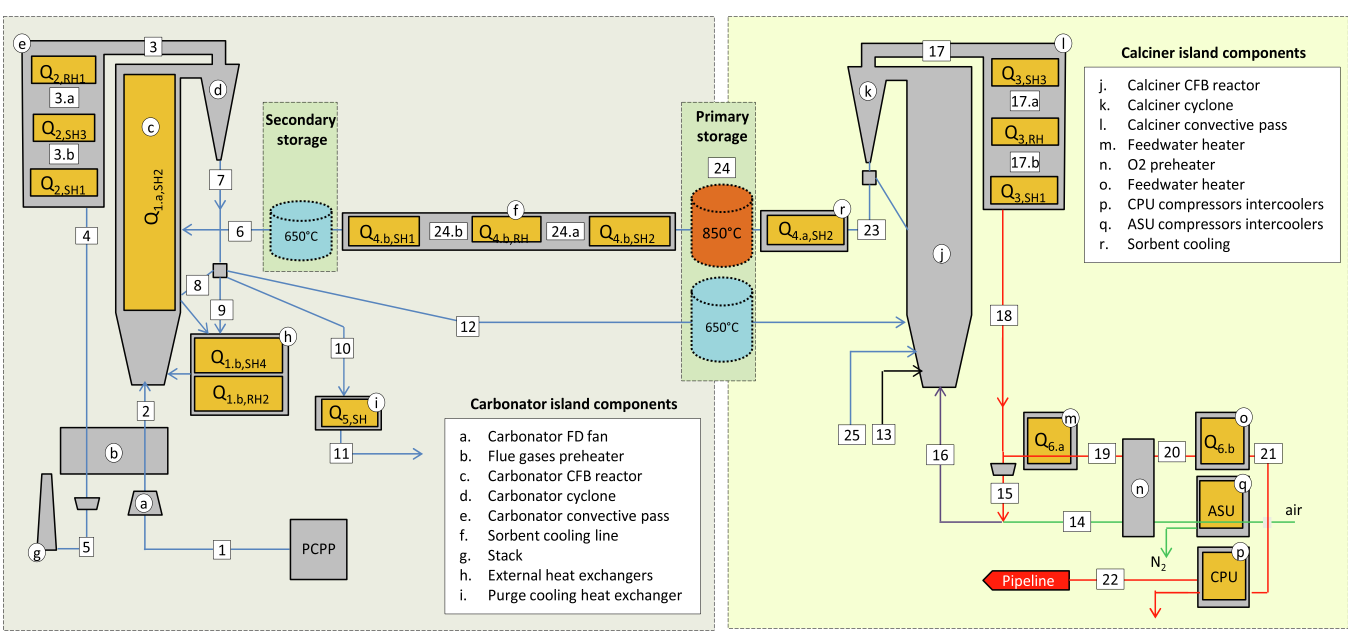


**Fig. 1.** Schematic of the CaL system with the arrangement and the nomenclature of the heat exchangers.

**Table 3**
Average steam cycle power output and flue gas mass flow rate of the PCPP for weekdays, weekend days and overall week calculated with respect to the full load quantities.

| | Mon-Fri | Sat-Sun | Week |
|---|---|---|---|
| PCPP gross power output | 74.1% | 37.6% | 63.7% |
| PCPP flue gases mass flow rate | 75.0% | 40.0% | 65.0% |

[33]. The main assumptions adopted are listed in Table 4 with some significant quantities resulting from the assumed values (e.g. reactor cross section derived from the assumed superficial velocity).

#### 2.1.1. Carbonator island

The carbonator line mainly comprises the carbonator reactor (c in Fig. 1) designed as a cooled circulating fluidized bed (CFB) reactor operating at 650 °C, the reactor convective pass (e), a system of cyclones, return legs and loop-seals for solid separation and recirculation (d) and a Ljungström flue gas pre-heater to improve the process efficiency (b).

In the carbonator, $CO_2$ is removed from the PCPP flue gas through the exothermic carbonation reaction ($CaO + CO_2 \rightarrow CaCO_3$). Desulfurized flue gas from the PCPP (stream #1) is blown by fan (a), enters at the bottom of the carbonator reactor after preheating up to 300 °C (#2) in the Ljungström gas–gas heater (b) while CaO-rich solids (#6) are provided at 650 °C after cooling in the sorbent cooling line (f + r).

Cyclones at the top of the carbonator (d) separate solids (#7) from gas (#3). $CO_2$-lean gas is cooled (#4) in the carbonator convective pass (e) and after flue gas preheating is released (#5) to the stack (g). Different cyclone efficiency has been assumed for Ca-based solids (99.9%) and ash (90%), considering to exploit the different average particle size of sorbent and fuel fed to the calciner to have a selective separation of the solids [39]. Sorbent derives from limestone make-up ($F_0$) and is assumed to be fed with an average particle size of around 200 µm, while pulverized coal with particle size of around 20 µm is assumed to be combusted in the calciner. Carbonated solids from the cyclone (#7) are split in four streams by a system of loop seals: a fraction is recirculated to the reactor (#8), a fraction (#9) is cooled in a series of bubbling bed external heat exchangers (EHE) (h), a fraction is purged (#10) and cooled in a dedicated heat exchanger (i) and a fraction is sent to the calciner island (#12).

**Table 4**
Main assumptions for the design of the CaL system and some calculated quantities labelled with (*). Carbonator global heat transfer coefficient is derived from [38].

| | |
|---|---|
| **Carbonator island** | |
| Operating temperature, °C | 650 |
| Riser global heat transfer coefficient, $W/m^2K$ | 200 |
| Riser height, m | 20 |
| Inventory, $kg/m^2$ | 1000 |
| $F_0/F_{CO2}$, - | 0.1 |
| $CO_2$ capture efficiency, % | 90 |
| Mean gas superficial velocity, m/s | 5 |
| Pressure loss in nozzles, bed and cyclone, kPa | 12 |
| Pressure loss in convective pass, kPa | 3.5 |
| Pressure loss in gas-gas heater, kPa | 1 |
| Gas temperature at convective pass outlet, °C | 350 |
| (*) $F_{Ca}/F_{CO2}$, - | 7.01 |
| (*) Cross section, $m^2$ | 430 |
| **Calciner island** | |
| Operating temperature, °C | 920 |
| Riser height, m | 20 |
| Mean gas superficial velocity, m/s | 5 |
| Oxygen concentration in oxidant stream, $\%_{vol}$ | 50 |
| Pressure loss in nozzles, bed and cyclone, kPa | 20 |
| Oxygen concentration in $CO_2$-rich gas, $\%_{vol}$ | 5 |
| Recycle gas temperature, °C | 350 |
| Pressure loss in the convective pass, kPa | 3.5 |
| (*) Cross section, $m^2$ | 215 |
| **Auxiliaries** | |
| Cyclones efficiency on Ca species, % | 99.9 |
| Cyclones efficiency on ash, % | 90 |
| Fans isentropic efficiency, % | 80 |
| Fans electric-mechanical efficiency, % | 94 |
| Coal milling and handling systems, $kJ_e/kg_{coal}$ | 50 |
| Limestone handling systems, $kJ_e/kg_{limestone}$ | 90 |
| Purge handling systems, $kJ_e/kg_{purge}$ | 100 |
| **Air Separation Unit (ASU)** | |
| Oxygen purity, $\%_{vol}$ | 95 |
| Electric consumption, $kWh_e/t_{O2}$ | 160.0 |
| Heat for TSA bed regeneration, $kJ_{th}/kg_{O2}$ | 18.3 |
| Pressure of steam for TSA bed regeneration, bar | 8 |
| **$CO_2$ compression and purification unit (CPU) (Aspen Plus)** | |
| Final $CO_2$ pressure, bar | 110 |
| Number of LP/HP intercooled compression stages, - | 3/2 |
| Compressor isentropic efficiency LP/HP, % | 81 / 83 |
| LP intercooled compressors pressure ratio | 18.1 |
| HP intercooled compressors pressure ratio | 6.3 |
| Final pump pressure increase, bar | 21 |
| Temperature in the $CO_2$ purification vessel, °C | −54 |
| Multi stream heat exchanger ΔT pinch point, °C | 2 |
| (*) Final $CO_2$ purity, % | 95.7% |
| (*) Electric consumption, $kWh_e/t_{CO2}$ | 115.8 |
| (*) fraction of vented $CO_2$ with non-condensable gas | 3% |

#### 2.1.2. Calciner island

The calciner island comprises the calciner reactor (j) designed as a refractory lined CFB reactor operating at 920 °C, a convective pass (l), the ASU (q) for the production of high purity oxygen and the CPU (p).

In the calciner (j), fresh limestone (#25) is fed to maintain adequate sorbent activity in the system. In this reactor all $CaCO_3$, whether from the carbonator (#12) or from the make-up (#25), is converted to CaO and a concentrated stream of $CO_2$ is released (#17). Heat for the endothermic calcination reaction ($CaCO_3 \rightarrow CaO + CO_2$) and for heating the solids to the calcination temperature is provided by the oxy-combustion of pulverized coal (#13).

After solids separation by cyclones (k), $CO_2$-rich flue gas (#17) is cooled in the calciner convective pass (l) down to 350 °C (#18) and partially recirculated (#15) and mixed with high purity oxygen (#14) to achieve an $O_2$ concentration of $50\%_{vol}$ at the calciner inlet (#16). The remaining portion (#19) is further cooled down to close ambient temperature in a series of heat exchangers (m, n, o), preheating CaLPP feedwater and the high purity oxygen (#14), and it is eventually compressed and purified (#21) in the CPU (p) and delivered to a pipeline (#22) for $CO_2$ transport and storage. Hot CaO-rich solids (#23) are cooled in dedicated fluidized bed sorbent cooling heat exchangers (f + r) and returned to the carbonator.

### 2.2. Storage system

The *Baseline* case does not include any storage unit and it represents the classic CaL configuration for $CO_2$ capture retrofit in a coal-fired power plant [40,41], where the sorbents circulates between the carbonator and the calciner with no intermediate storage. In this configuration both reactors of the CaL system (and all the auxiliary components, such as the ASU and the CPU) are sized on the peak load of the PCPP to ensure high $CO_2$ capture efficiency at any load and their operation simply follows the PCPP load variation. On the contrary, the *FlexiCaL* plant is provided with refractory silos for solids storage allowing the solid streams coming from both reactors to be stored at different temperatures. The use of hot solids storage may be attractive for two different reasons and for this case two different storage systems are considered (Fig. 1): a primary storage system for calciner line downsizing and a secondary storage system to improve the flexibility of the system.

- The primary storage system allows to decouple the operation of the calciner island from the operation of the carbonator island which follows the PCPP load. In this way, the calciner island (i.e. calciner with associated heat recovery, ASU and CPU) is downsized and work with high capacity factor, experiencing smaller load fluctuations. Two silos are required, as reported in Fig. 1: the low temperature vessel (650 °C) is used to store the excess of $CaCO_3$-rich solids produced by the carbonator when the carbonator load is higher than the calciner one; the high temperature vessel (850 °C) stores CaO-rich solids when the carbonator load is lower than the calciner one. Hot storage tank temperature is assumed equal to 850 °C (i.e. lower than the calciner outlet temperature of 920 °C) in order to reduce deactivation of the sorbent due to prolonged time at high temperature. For this analysis, the calciner island has been sized on the weekday average capacity factor, namely at the 75% of the *Baseline* case, which represents the optimal case from a technical-economic perspective, as estimated in [33].
- A secondary smaller volume silo can be placed between the end of the sorbent cooling line and the carbonator inlet (Fig. 1). This secondary storage system can be used to provide the system with increased flexibility, by allowing quick variation of power output by controlling the fluidization of the solid heat exchangers between hot primary storage tank and secondary storage tank. If high temperature storage tank is not empty and a power output increase is required, solids mass flow rate from primary storage hot tank to secondary storage vessel can be increased by boosting the fluidization of the sorbent cooler line. This results in an increase of thermal power available for the CaLPP and thus an increase of power output with respect to the nominal value. On the contrary, if the hot primary storage is not completely full and a rapid power reduction is required, it is possible to interrupt the flow of solids along the sorbent cooler line and ensure the correct operation of the carbonator by exploiting the solids previously accumulated in the secondary storage system. This would also allow to reduce the minimum load of the CaLPP system. Therefore, this additional storage system allows fast power output variations acting on the fluidization of the sorbent cooling line without affecting the CaL reactors operation, providing the opportunity to play on the highly remunerated secondary electricity market without involving a reduction of $CO_2$ capture efficiency.

### 2.3. CaL power plant (CaLPP)

CaL system releases a large amount of heat at different temperatures that is used as heat input in a supercritical steam power plant. High temperature heat (≥350 °C), that can be used for live steam production and steam reheating, is available from the carbonator waterwalls (c), the external heat exchangers (h), the carbonator off gas cooling (e), the sorbent coolers (f, r), the calciner off gas cooling (k) and the solids purge (i). The remaining thermal power is available from medium and low temperature sources (<350 °C) and it is used for feedwater preheating. $CO_2$ cooling (m) is the only source at medium temperature (≥150 °C), while low temperature heat is available from $CO_2$ coolers (o), ASU (q) and CPU (p) compressors recuperative intercoolers, where hot gas is available at 140 °C. CaLPP has been designed in ThermoFlex [42] as a USC steam cycle using the set of assumptions reported in Table 5.

**Table 5**
CaLPP steam cycle assumptions adopted in Thermoflex simulations.

| Steam cycle | |
|---|---|
| Boiler feed water temperature, °C | 307 |
| Boiler feed water pressure, bar | 320 |
| SH/RH live steam temperature, °C | 560/580 |
| SH/RH live steam pressure, bar | 270/56 |
| SH/RH pressure loss at turbine admission valve, % | 2 |
| RH pressure loss, bar | 4 |
| Condensing pressure, bar | 0.048 |
| Number of preheaters (including the deaerator) - | 6 |
| Pinch-point ΔT in FWHs, °C | 3 |
| Steam pressure loss in deaerator/surface FWHs, % | 7/3 |
| Steam turbine rotational speed, rpm | 3000 |
| Steam turbine number of HP/IP/LP parallel flows - | 1/2/4 |

Fig. 2 shows the arrangement of the heat exchangers along the water path in the different sections of the CaL system. The following comments can be made on the selected power plant design:

- The CaLPP steam parameters 560/580 °C and 270/56 bar are in line with the Lagisza CFB supercritical coal power plant [43].
- High pressure steam is produced in three parallel lines, labeled with SH, (carbonator, calciner and sorbent cooling namely streams 128, 121, 125 as reported in Fig. 2) plus the heat recovered from the solids purge (stream 120). Steam is reheated in three parallel lines, labeled with RH, (carbonator, calciner and sorbent cooling namely streams 136, 141, 139 in Fig. 2). Heat exchangers for generation of superheated and reheated steam are arranged with the aim of reducing the tube wall temperature without incurring in heat recovery limitation due to pinch point within the heat exchangers. The temperature-heat diagram of the overall heat recovery is shown in Fig. 3 for the *Baseline* case. Using the same thermodynamic point enumeration of Fig. 2, numbers indicate the connection points between the various heat exchanger banks for live steam production and steam reheating. For example, in the calciner line, water from the high pressure preheating line at 307 °C and 320 bar (#121) is first heated to 420 °C (#122) recovering the heat from the $CO_2$ rich gases ($Q_{3,SH1}$), then superheated to 500 °C (#123) exploiting the heat of CaO-rich solids from 920 °C to 850 °C ($Q_{4,a,SH2}$) and finally sent to the high temperature convective section of the calciner ($Q_{3,SH3}$) to reach the final temperature of 560 °C (#124). The remaining part of the heat available from the $CO_2$-rich stream ($Q_{3,RH}$) is used to reheat the steam (from #141 to #142). Similar observations can be made for the sorbent cooling line, where high pressure steam and reheated steam are generated using the heat released by the CaO-rich solids between 850 °C and 650 °C. Sorbent purge is a minor source of high temperature heat (around 0.3% of the total) and it has been modelled as a single pure counterflow fluidized bed heat exchanger for live steam production. Differently, a more complex arrangement is required for the carbonator line as discussed in detail below.
- Heat is recovered by the carbonator reactor from carbonator waterwalls (c) and external heat exchangers (h). The higher the heat transfer area in the riser, the lower the duty of the external heat exchangers. The controllability of the heat exchanged in the two sections is very different. The heat transfer area and the heat flux inside the riser cannot be controlled at part-load. On the contrary, the thermal power transferred in the external fluidized bed heat exchangers can be controlled by modifying their fluidization and by bypassing the solids from the cyclone, as proposed in the Foster Wheeler “INTREX” design [44]. At part-load, the carbonator reactor bed temperature should remain as close as possible to the nominal value of 650 °C in order to limit sorbent deactivation at low temperature [45] and to reduce the consumption of coal and oxygen for sorbent heating in the calciner. Therefore, to allow a high turn-down ratio while keeping the target temperature in the carbonator, the heat transfer surface should be preferably placed in the external heat exchangers rather than in the riser. This has been obtained by installing only membrane waterwalls and avoiding additional heat transfer surface inside the riser (e.g. wingwalls, platens, full height internal walls) and by adopting a relative low height for the carbonator (20 m), which is sufficient to achieve a high $CO_2$ capture efficiency without increasing the cooled lateral surface area more than needed.
- CaLPP steam cycle also recovers heat for water preheating. A large fraction of the low temperature heat for condensate preheating (from #102, #103 to #104, #105) is recovered from the $CO_2$ cooling (o)

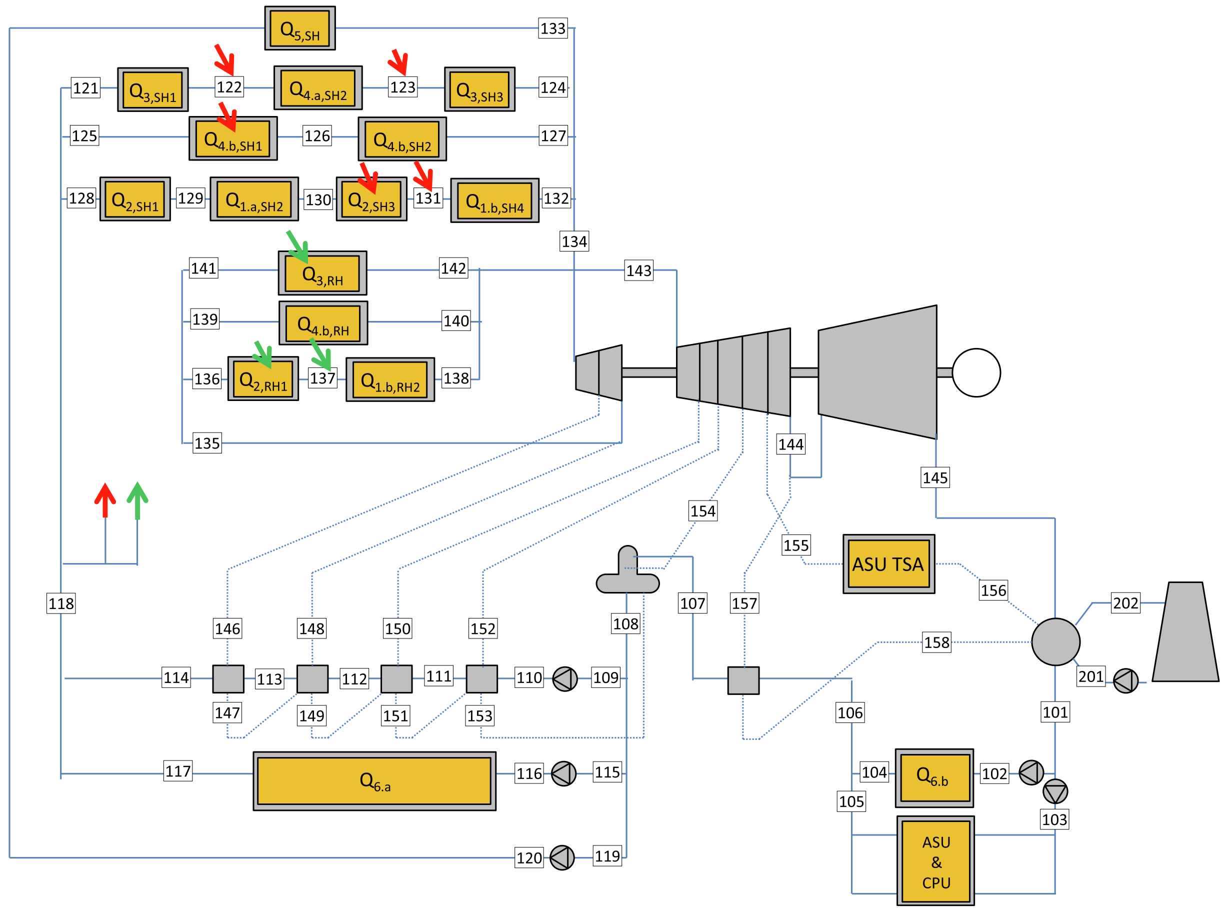


**Fig. 2.** Arrangement of the heat exchangers in the CaL system with reference to the water path. Red and green arrows show the position of the attemperation/desuperheating in the SH and RH lines respectively. It must be noted that "SH" is here used to generally indicate the high pressure heating lines, also comprising economizer and evaporators.

and the recuperative intercoolers of the ASU (q) and CPU (p) compression trains. In both the *Baseline* and *FlexiCaL* cases the waste heat available at low temperature is sufficient to preheat the whole condensate mass flow rate up to 120 °C, avoiding steam bleeding from the turbine. A single low pressure regenerative feed water heater (FWH) fed by a dedicated steam bleeding is placed before the deaerator which is operated at 9.7 bar. High pressure FWHs (from #116 to #117) recover heat from $CO_2$ cooling (m) between the recycle split and the oxygen preheater (n). In addition, four high pressure FWHs are adopted (from #110 to #114). The final water preheating temperature is equal to 307 °C.

- From the intermediate pressure turbine, a small fraction of steam is bled for regeneration of the TSA beds of the ASU. The condensate flow is then returned to the condenser.

## 3. Methodology for part-load analysis

Part-load performance of both *Baseline* and *FlexiCaL* cases has been evaluated using Thermoflex software [42] on a grid of different off-design conditions representing the possible operating conditions of the system during a representative year. The set of part-load points analyzed is different for the two cases, as shown in Table 6:

- *Baseline* case is not provided with storage system and both reactors work at the same load in off-design. Four cases with a PCPP flue gases mass flow rate ranging from 40% to 100% of the nominal load are investigated. PL40 case is representative also of weekend operation;
- *FlexiCaL* case is provided with both storage systems. For the primary storage system, a silo size sufficient to guarantee stable daily operation of the calciner line has been selected. This corresponds to a calciner island with 75% size of the *Baseline* case, i.e. the weekday average capacity factor. Weekday part-load operations are thus characterized by PCPP flue gases mass flow rate ranging from 40 to 100% of the nominal one, with the calciner island working always at its nominal load (i.e. 75% of the calciner load in the *Baseline* case). In addition, the operating week-end minimum (WE-MIN) condition is considered, where the calcined sorbent silo is full and the calciner load is reduced to match the PCPP load, corresponding to a relative load of 0.40/0.75 = 53%. Furthermore, two additional operating conditions are studied exploiting the potential of the secondary storage:
  i. DES-HIGH: typical weekday condition with the PCPP running at nominal load and a request of additional power output. This condition is simulated with the carbonator and the calciner at their nominal load, by increasing the solid mass flow rate from the hot solid vessel by 30% and by storing the cooled solids in the secondary vessel at carbonator inlet. In this way, the heat input to the CaLPP steam cycle and its power output are rapidly increased while the high temperature storage is emptied.
  ii. PL40-LOW: typical weekday condition with the PCPP running at minimum load and a request to further reduce the power output. This condition is simulated with the carbonator at minimum load (40%) and the calciner at its nominal load, by interrupting the flow of solids through the heat exchangers between the primary storage hot vessel and the secondary storage tank. In this way, the

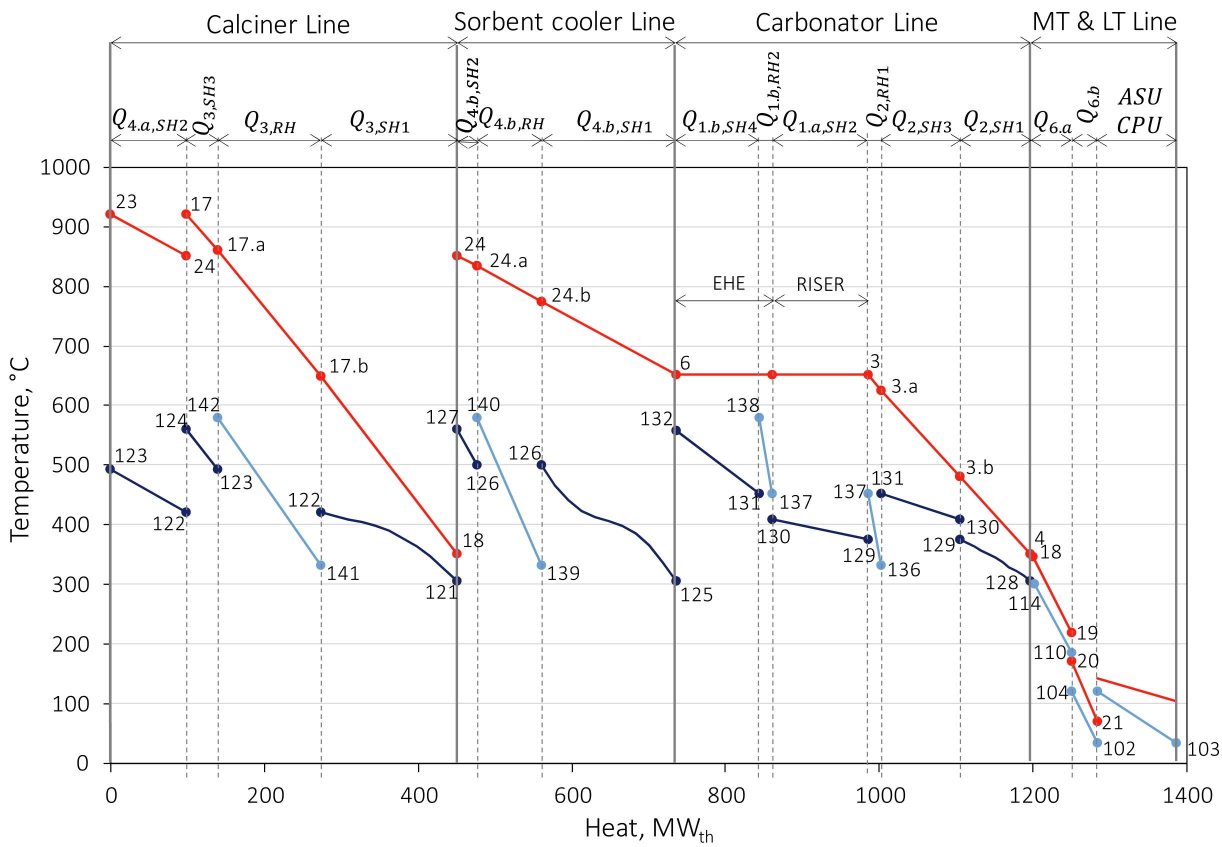


**Fig. 3.** Temperature-heat diagram for *Baseline* case where it is possible to highlight the complex heat exchanger disposition in the three main high temperature lines for live steam production (SH) and steam reheating (RH). Purge cooling ($Q_{5,SH}$) is a minor source of heat (around of 0.3% of the total) and is not presented in the figure. *FlexiCaL* case can be obtained reducing by 25% the amount of heat available from calciner line and MT&LT line ($CO_2$ cooling, ASU and CPU).

power output rapidly drops while the primary storage hot silo is filled.

The size of the secondary storage silo affects the maximum duration of the DES-HIGH and PL40-LOW operating conditions. However, as ancillary services on the balancing market are requested for a limited amount of time (e.g. from few minutes to 15 min), the secondary storage tank is expected to have a considerably lower volume than the primary storage.

To solve the heat and mass balances at part-load for each investigated condition, two aspects need to be discussed in the next sections: (i) the modelling approach of the plant components at part-load and (ii) the selected control strategy

### 3.1. Modelling approach of the plant components at part-load

Each component is controlled in off-design with the strategies summarized below:

- The first stage of the high pressure steam turbine is controlled by partial arc admission and, for the sake of simplicity, we assumed an infinite number of sectors and a smooth control of the turbine

**Table 6**
Part-load conditions investigated in this work: Cases with exploitation of secondary storage are labelled with (*). PCPP flue gas mass flow rate ratio (FG Ratio) is defined with respect to the nominal one. Component duty ratio (Duty Ratio) is defined with respect to same component nominal duty in *Baseline* case.

| | FG Ratio | Duty Ratio | | |
|---|---|---|---|---|
| | | Carbonator island | Calciner island | Sorbent cooler 850 °C-650 °C |
| Baseline case | | | | |
| DES | 100% | 100% | 100% | 100% |
| PL80 | 80% | 80% | 80% | 80% |
| PL60 | 60% | 60% | 60% | 60% |
| PL40 | 40% | 40% | 40% | 40% |
| FlexiCaL case | | | | |
| DES-HIGH* | 100% | 100% | 75% | 130% |
| DES | 100% | 100% | 75% | 100% |
| PL80 | 80% | 80% | 75% | 80% |
| PL60 | 60% | 60% | 75% | 60% |
| PL40 | 40% | 40% | 75% | 40% |
| PL40-LOW* | 40% | 40% | 75% | 0% |
| WE-MIN | 40% | 40% | 40% | 40% |

admission, capable to always keep a constant admission pressure. This also means that the turbine nozzle must be sized with a swallowing capacity corresponding to the maximum mass flow rate, that in the *FlexiCaL* case occurs in the DES-HIGH operating point. All the others turbine stages are designed as full admission stages with uncontrolled inlet pressure. The efficiency of each group of turbine stages is computed in off-design with Thermoflex built-in correlations.
- Pumps are equipped with variable speed motor.
- Most of the heat exchangers are directly designed by Thermoflex and are calculated at part-load by means of built-in correlations for pressure drops and heat transfer coefficients, depending on the fluids flow rate and the heat exchanger geometry.
- The heat exchangers in the carbonator hot loop (riser and external heat exchangers) are calculated with the following method:
  - o For the carbonator riser, a constant global heat transfer coefficient has been assumed in agreement with [38], that shows very small dependency on the load of large CFB boilers.
  - o The thermal power transferred in the carbonator external heat exchangers is tuned by controlling their fluidization [44]. This feature is implemented in Thermoflex by tuning the UA of the external heat exchangers, down to a minimum UA = 0, corresponding to complete deactivation through bypass of solids.
  - o The water side pressure drops are modified in off-design operations as function of the actual mass flow rate, considering the off-design behaviour calculated by Thermoflex on similar heat exchangers. After a simple model calibration, the pressure drops have been assumed proportional to the mass flow rate at the 1.265 power ($m^{1.265}$).

### 3.2. Part-load control strategies

To obtain feasible off-design steady state solutions as representative of the real CaLPP performance, the following control strategies have been implemented in the model:

- *Sorbent handling.* Fresh sorbent make-up ratio $F_0/F_{CO2}$ and sorbent circulation ratio to the carbonator $F_{Ca}/F_{CO2}$ are kept constant. This is obtained by keeping the fresh sorbent (#25 in Fig. 1) and recirculated sorbent (#6) flow rates proportional to flue gas mass flow rate from the PCPP. The purge mass flow rate (#10) is also proportional to the carbonator load.
- *Steam mass flow rate*. The SH and RH mass flow rates are split among the different heat exchangers of the calciner and hot solid heat exchanger lines with the aim of limiting steam desuperheating/attemperation need. Controlling valves are positioned at the beginning of each superheating and reheating line in order to control the steam mass flow rate in each branch. Steam attemperation is required in different sections of the system especially at low loads to avoid tube overheating. Pressurized water for superheated and reheated steam attemperation is derived after the last FWH outlet as shown in Fig. 2.
- *Carbonator island control.* The system is controlled to avoid the decrease of the reactor temperature, in order to limit sorbent deactivation and avoid an increase of the sensible heat to be provided in the calciner for sorbent heating. This involves an increase of the average water temperature in the carbonator riser, since the reduced thermal power (roughly proportional to the PCPP flue gas flow rate) is transferred with a constant UA, leading to a reduction of the average temperature difference between the solids in the riser and the water in the waterwalls. The target live steam (#132) and reheated steam (#138) temperatures are then obtained by controlling the heat transfer rate in the external heat exchangers, which are dedicated to final SH and RH.
- *Hot solid mass flow rate and temperature control.* The terminal solid temperatures from solid heat exchangers are set equal to the nominal value: 850 °C (#24) and 650 °C (#6) to avoid temperature variation in the storage tanks. The temperature in #24 is controlled by adjusting the temperature of steam coming from $Q_{3,SH1}$, while the temperature in #6 is controlled by adjusting the mass flow rate of steam passing through the high-pressure branch of the sorbent cooler line. Only in the DES-HIGH of the *FlexiCaL* case it is not possible to match the target on the temperature of solids entering in the secondary storage vessel (#6): minimum solid temperature in this case is slightly higher than 650 °C because the increased heat duty leads to under-sized heat transfer area of solid heat exchangers (f) which work with larger average temperature differences.
- *Calciner island control.* The consumption of coal (#13) and oxygen (#14) is proportional to the $CaCO_3$-rich solids (#12) mass flow rate fed to the calciner. This allows to keep the calciner exit temperature constant. The steam flow rate used for the ASU TSA (#154) and the low temperature heat available from ASU and CPU compressors intercoolers are proportional to the calciner load.
- *Steam cycle control.* The degree of admission of the high pressure steam turbine is adjusted as function of the live steam mass flow rate in order to keep the SH pressure and turbine inlet pressure equal to the nominal value at any load. This ensures that the high pressure heat exchangers do not work with a boiling fluid at low loads, avoiding possible issues related to metal skin over temperature. No pressure control is required for the other turbine stages, which work in sliding pressure, causing a decrease at part-load of: (i) the pressure and temperature of the steam bled for feed water heating, (ii) the reheating pressure, (iii) the crossover pressure and (iv) the deaerator pressure. The condenser is operated with a constant mass flow rate of cooling water, leading to a reduction of the condensation temperature at part-load.

## 4. Results and discussion

Results are presented in three sections. The first one discusses the components design of the two assessed cases and the energy balances at nominal load. The second focuses on part-load results, highlighting the differences between the two investigated cases and providing the interpretation of the trends of significant quantities vs. PCPP load. The third part discusses the economic performance of the different cases.

### 4.1. Nominal load operation and components design

The distribution of the available heat from the different sections of

**Table 7**
Temperatures and heat available in the different sections of the CaL plants at full load.

| | | T range $T_{max}$-$T_{min}$ °C | *Baseline* case Heat available | | *FlexiCaL* case Heat available | |
|---|---|---|---|---|---|---|
| | | | MW | % | MW | % |
| Carbonator riser and EHE | $\dot{Q}_2$ | 650–650 | 249.6 | 16.8 | 249.6 | 19.2 |
| Carbonator convective pass | $\dot{Q}_2$ | 650–350 | 211.9 | 14.3 | 211.9 | 16.3 |
| Purge cooler | $\dot{Q}_5$ | 650–231.5 | 5.2 | 0.3 | 5.2 | 0.4 |
| Calciner convective pass | $\dot{Q}_3$ | 920–350 | 352.5 | 23.8 | 264.4 | 20.3 |
| Calcined solids coolers HT | $\dot{Q}_{4.a}$ | 920–850 | 99.6 | 6.7 | 74.7 | 5.7 |
| Calcined solids coolers LT | $\dot{Q}_{4.b}$ | 850–650 | 284.6 | 19.2 | 284.6 | 21.9 |
| MT $CO_2$ cooler | $\dot{Q}_{6.a}$ | 350–217.4 | 48.7 | 3.3 | 36.5 | 2.8 |
| LT $CO_2$ cooler | $\dot{Q}_{6.b}$ | 171.3–70 | 35.6 | 2.4 | 26.7 | 2.1 |
| LT ASU and CPU intercoolers | $\dot{Q}_7$ | 140–57 | 195.3 | 13.2 | 146.5 | 11.3 |
| Total | | | 1482.9 | | 1300.0 | |

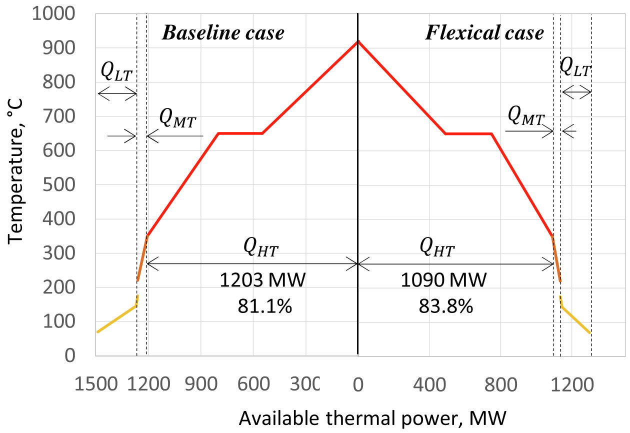


**Fig. 4.** Cumulative T-Q diagrams of the available heat for *Baseline* case (left) and *FlexiCaL* case (right).

the assessed CaL systems is reported in Table 7, while Fig. 4 depicts the cumulative temperature-heat diagram of the CaL system available heat sources. For both cases, the two main sources of high temperature heat for live steam production and steam reheating are the calciner off-gas cooling from 920 °C and 350 °C ($Q_3$) and the sorbent cooling between 850 °C and 650 °C ($Q_{4b}$), which represent 29.3% and 23.6% of the total high-temperature heat for the *Baseline* case and 24.2% and 26.1% for *FlexiCaL* case, respectively. Other significant thermal power is available from the carbonator waterwalls plus carbonator external heat exchangers ($Q_1$) and from the carbonator convective pass ($Q_2$).

The ratio between the high temperature heat available from the carbonator and the calciner lines differs because of the different sizing of the calciner island: high temperature heat from the carbonator island is 38.3% of the high temperature heat in the *Baseline* case and 42.3% in the *FlexiCaL* case. In both cases, less than 20% of the total available heat is released at medium–low temperature. In the *FlexiCaL* case, this quantity is lower than in the *Baseline* case (16.2% vs 18.9%) due to the lower amount of $CO_2$-rich gas mass flow rate released from the calciner and the downsizing of the ASU and the CPU. In spite of this difference, heat is sufficient for feedwater and condensate preheating. Additional information is available in the supplementary material section: in particular the properties of the gaseous and solid streams of the CaL systems at design (DES) conditions (Fig. 1) are reported in Table SI-1 and Table SI-2 while the thermodynamic properties of the CaLPP streams (Fig. 2) are reported in Table SI-3. The power balance of the PCPP + CaL plant and the key performance indicators are shown in Table 8. For the *Baseline* case, about 45% of the total fuel input is consumed in the calciner of the CaL plant. The CaLPP steam turbine generates additional 641.7 $MW_e$. The main additional auxiliary consumptions are associated to the CPU (122.1 $MW_e$), the ASU (70.6 $MW_e$), the power block auxiliaries (34.9 $MW_e$), the calciner auxiliaries (13.4 $MW_e$) and the carbonator fans (12 $MW_e$). The resulting net power output is 376.1 $MW_e$, corresponding to an increase of 50.3% with respect to the existing PCPP. The overall net electric efficiency of the PCPP + CaL plant is 37%, with an efficiency penalty of 7.54% points with respect to the existing PCPP without $CO_2$

**Table 8**
Power balance of the PCPP + CaL plant and key performance indicators for PCPP, *Baseline* and *FlexiCaL* cases operating at design conditions.

| | PCPP | Baseline case | FlexiCaL case |
|---|---|---|---|
| Carbonator $CO_2$ capture efficiency, % | – | 90.0 | 90.0 |
| $F_0/F_{CO2}$ | – | 0.1 | 0.1 |
| $F_{Ca}/F_{CO2}$ | – | 7.0 | 7.0 |
| *Electric Power Balance, MW* | *Only PCPP* | *Only CaLPP* | *Only CaLPP* |
| Steam turbine | 804.8 | 641.7 | 580.7 |
| Boiler feed water pump | −26.24 | −25.05 | −22.73 |
| Condensate extraction pump | −0.64 | −0.79 | −0.68 |
| Condenser auxiliaries | −6.25 | −9.05 | −8.20 |
| Auxiliaries for heat rejection (other than condenser) | – | −0.71 | −0.53 |
| Coal milling and handling | −3.33 | −2.53 | −1.90 |
| Filters and ash handling* / Purge and limestone handling** | −1.88 | −4.78 | −4.78 |
| Flue gas desulfurizer | −3.33 | – | – |
| Primary air FD fan* / Carbonator FD fan** | −1.26 | −11.97 | −11.97 |
| Secondary air FD fan* / $CO_2$ recirculation fan** | −2.20 | −5.36 | −4.02 |
| Boiler ID fan* / Carbonator ID fan** | −9.98 | −2.83 | −2.83 |
| ASU | – | −70.61 | −52.96 |
| CPU | – | −122.10 | −91.58 |
| BOP | −2.51 | −9.80 | −8.55 |
| Net electric power output, MW | 747.2 | 376.1 | 370.0 |
| Coal input, kg/s | 66.61 | 53.92 | 40.44 |
| Coal thermal input, $MW_{LHV}$ | 1676.5 | 1357.2 | 1017.9 |
| *Overall KPIs* | *PCPP* | *PCPP + CaLPP* | *PCPP + CaLPP* |
| Total gross power output, MW | – | 1446.5 | 1385.5 |
| Total net power output, MW | – | 1123.3 | 1117.2 |
| Total fuel consumption, $MW_{LHV}$ | – | 3033.7 | 2694.4 |
| Gross electric efficiency, $\%_{LHV}$ | 48.01 | 47.68 | -*** |
| Net electric efficiency, $\%_{LHV}$ | 44.57 | 37.03 | -*** |
| Net electric efficiency penalty, %pts. | – | −7.54 | -*** |
| Direct $CO_2$ emission at stack, kg/s | 162.5 | 16.2 | 16.2 |
| $CO_2$ vented from the CPU, kg/s | – | 8.8 | 6.6 |
| $CO_2$ specific emission, kg/MWh | 782.7 | 80.1 | -*** |
| $CO_2$ avoided, % | – | 89.8 | -*** |
| SPECCA, $MJ_{LHV}/kg_{CO2}$ | – | 2.34 | -*** |

* Items referred to the PCPP plant.
** Items referred to the *Baseline* and *FlexiCaL* CaL plants.
*** The *FlexiCaL* design operating point involves an excess of $CaCO_3$ production and the storage of carbonated sorbent. Therefore, the computation of efficiencies, specific emissions and SPECCA on such data is meaningless. KPIs of *FlexiCaL* case must be computed on complete operating cycles ending with unchanged state of charge of the storage system.

**Table 9**
Main results of the sizing of the heat exchangers steam generation and reheating of the *Baseline* case.

| | Duty, MW | Internal heat transfer coefficient, W/m$^2$-K | External heat transfer coefficient, W/m$^2$-K | Overall heat transfer coefficient, W/m$^2$-K | Area, m$^2$ | Material, - | Volume, m$^3$ | Weight dry, kg |
|---|---|---|---|---|---|---|---|---|
| $Q_{1.a,SH2}$ | 124.92 | – | – | 200 | 2470 | CS | 7540 | 126,543 |
| $Q_{1.b,SH4}$ | 107.22 | – | – | 400 | 1854 | T91 | 30 | 147,664 |
| $Q_{1.b,RH2}$ | 17.45 | – | – | 400 | 352 | T91 | 20 | 11,996 |
| $Q_{2,SH1}$ | 91.04 | 9137 | 94 | 88 | 15,064 | CS | 1176 | 926,500 |
| $Q_{2,SH3}$ | 102.87 | 10,884 | 100 | 86 | 10,195 | T22 | 760 | 1,121,000 |
| $Q_{2,RH1}$ | 17.97 | 1516 | 101 | 83 | 882 | T22 | 57 | 84,500 |
| $Q_{3,SH1}$ | 177.80 | 16,255 | 119 | 109 | 17,308 | CS | 1022 | 1,137,000 |
| $Q_{3,RH}$ | 134.81 | 1468 | 142 | 120 | 3771 | T91 | 219 | 146,400 |
| $Q_{3,SH3}$ | 39.94 | 3619 | 167 | 137 | 803 | T91 | 27 | 63,900 |
| $Q_{4.a,SH2}$ | 99.60 | – | – | 400 | 581 | T22 | 8 | 44,508 |
| $Q_{4.b,SH1}$ | 174.78 | – | – | 400 | 1410 | T22 | 34 | 76,947 |
| $Q_{4.b,RH}$ | 84.29 | – | – | 400 | 622 | T91 | 25 | 21,126 |
| $Q_{4.b,SH2}$ | 25.48 | – | – | 400 | 204 | T91 | 13 | 15,723 |
| $Q_{6,a}$ | 48.69 | 10,536 | 80.2 | 44 | 27,385 | CS | 222 | 351,520 |
| $Q_{6,b}$ | 33.56 | 3697 | 60.95 | 58 | 13,035 | CS | 961 | 460,550 |
| $O_2$ preheater (n) | 16.08 | 56.89 | 47.08 | 25 | 6578 | CS | 260 | 101,900 |

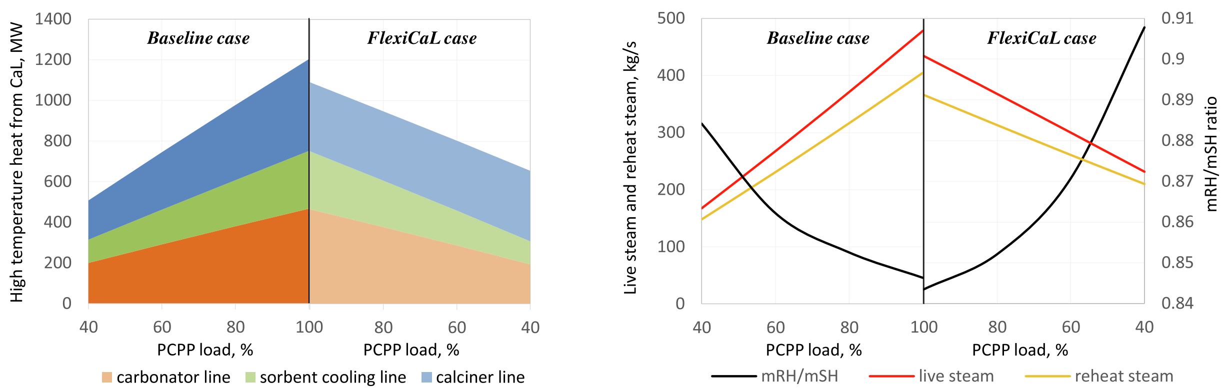


**Fig. 5.** (left) high temperature heat share as function of the PCPP load; (right) live steam, reheated steam mass flow rate and $m_{RH}/m_{SH}$ as function of PCPP load.

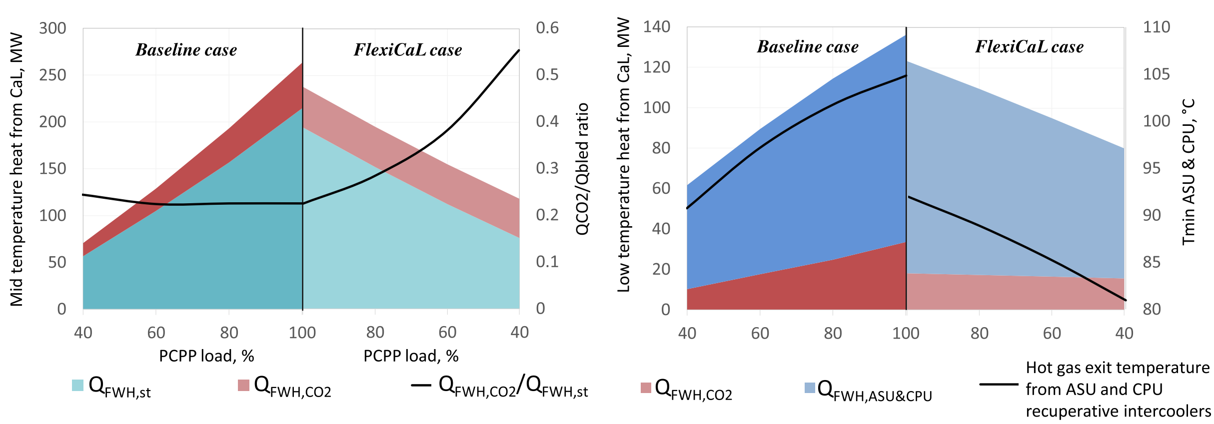


**Fig. 6.** (left) medium temperature heat share and $Q_{FWH,CO2}/Q_{FWH,st}$ ratio as function of the PCPP load, (right) low temperature heat share and hot gas exit temperature from CPU and ASU compressors recuperative intercoolers as function of the PCPP load.

capture, calculated with consistent assumptions. The total $CO_2$ emissions of the plant are 80.1 kg/MWh, corresponding to a $CO_2$ avoidance of 89.8% compared to the reference PCPP. The specific primary energy consumption for $CO_2$ avoided (SPECCA) is 2.34 $MJ_{LHV}$/kg. For the *FlexiCaL* case, the size of the CaL system is smaller and this leads to lower steam turbine power output (580.7 $MW_e$) and lower power block auxiliary consumption. However, downsizing of the calciner island allows to obtain a net power output of only 6.1 $MW_e$ less than the *Baseline* case. It must be observed that the overall performance indicators of the *FlexiCaL* case cannot be evaluated on a single operating condition where storage silos are loaded/unloaded, but must be calculated on a complete cycle with the same initial and final state of charge of the storage silos as reported in section "Cyclic energy balance".

Table 9 reports the preliminary sizing results for all the heat exchangers for live steam production and steam reheating for the *Baseline* case. The components of the calciner line (labelled by *) of the *FlexiCaL* case can be roughly obtained by reducing duty, area, volume and weight by 25% with respect to the tabulated values. The design of all the

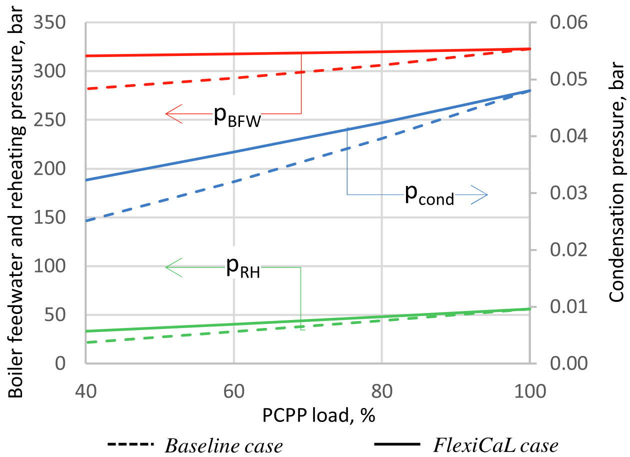


**Fig. 7.** trend of boiler feedwater pressure ($p_{BFW}$), reheating pressure ($p_{RH}$) and condensation pressure ($p_{cond}$) as function of the PCPP load.

components of the steam cycle, namely the steam turbine assembly, the condenser and the regenerative FHWs is carried out in Thermoflex and reported in the supplementary information of this paper (Tables from SI-4 to SI-9).

The primary storage of *FlexiCaL* case must accommodate the surplus of calcined material produced by the calciner island during PCPP low load operations. Two vessels with 31 m diameter and 16 m high (aspect ratio H/D of 0.5 assumed) are required. The secondary storage vessel is designed to accommodate a 30% increase of sorbent flow rate for 15 min operation. It results in a volume of around 1.4% of the overall primary storage, corresponding to a tank of around 7.5 m in both diameter and height (aspect ratio H/D of 1 assumed).

### 4.2. Part-load performance

#### 4.2.1. System behaviour at part-load

Figs. 5, 6 and 7 depict the trend of the main CaLPP quantities for the different PCPP loads, comparing the results of the *Baseline* case (left side) and the *FlexiCaL* case (right side) without exploiting the secondary storage availability. The following observations can be made based on the results reported in these figures.

- The overall heat introduced in the CaLPP at high temperature (i.e. in economizer, superheaters and reheaters) decreases with the load of the PCPP (Fig. 5.left). For the *Baseline* case, the decrease of the flue gases mass flow rate released from the PCPP involves an almost proportional reduction of all the thermal power sources available from all the sections of the CaL system. At the minimum PCPP load (40%) the high temperature heat is around 42% of the nominal one since the convective pass heat exchangers result oversized at part-load and allow to increase the recovery of the off-gas sensible heat in both the calciner and the carbonator lines. The total amount of high temperature heat is lower at design conditions for the *FlexiCaL* case because of the lower size of the calciner island, but it shows a milder reduction at part-load, since the calciner line works with constant fuel input. As a result, the high temperature heat available in the *FlexiCaL* case is between 60% and 100% of the design value, vs. 42–100% in the *Baseline* case, involving a smaller variation in the part-load operating parameters of the associated CaLPP. The reduction of the available thermal power leads to a reduction of both superheated and reheated steam mass flow rates (Fig. 5.right), that is more marked in the *Baseline* case than in the *FlexiCaL* case. Another consequence of the different sizing criteria is the portion of heat available from the calciner line compared to the other sources, which does not change significantly in the *Baseline* case (about 38%), while increases from 31% at full load to 53% at minimum PCPP load in the *FlexiCaL* case.
- In the *Baseline* case, the reduction of the high temperature and medium–low temperature heat is homogeneous and the amount of heat provided in the high pressure FWHs by the bled steam ($Q_{FWH,st}$) remains roughly proportional to the heat from $CO_2$ cooling ($Q_{FWH,CO2}$). The small increase of the $Q_{FWH,CO2}/Q_{FWH,st}$ ratio at the minimum PCPP load is due to the increased effectiveness of the FWHs fed by $CO_2$ (Fig. 6.left). On the contrary, in the *FlexiCaL* case, the amount of heat available from $CO_2$ cooling from the outlet of the convective pass (#18) is nearly constant at any load, resulting in a progressive reduction of relative contribution of the FWH fed with the steam bleeding. As a result, at the minimum PCPP load, the heat from $CO_2$ cooling provides around 55% of the overall heat required in the high pressure FWHs, which is more than twice the heat required at nominal load (23%) (Fig. 6.left). This also leads to a larger mass flow rate in the intermediate and low pressure turbines and a higher RH/SH steam mass flow rate ratio at low loads (Fig. 5.right).

With the exception of the last FWH, the low pressure feedwater preheating line relies on the heat available from $CO_2$ cooling and the CPU and ASU compressors recuperative intercoolers (Fig. 6 right). At all load, the intercoolers hot gas inlet temperature is equal to 140 °C, while the outlet temperature depends on the feed water flow rate and on the off-design heat transfer law of the heat exchangers. At nominal load, the gas exit temperature from the intercoolers is higher in the *Baseline* case (105 °C) than in the *FlexiCaL* case (92 °C) because in the latter the lower $CO_2$ and air flow rate leads to a higher utilization of the heat available from the ASU and CPU. When the PCPP load is reduced, the gas exit temperature from the ASU and CPU recuperative intercoolers decreases because of the higher effectiveness of the FWHs.

- Fig. 7 depicts the trend of the pressure at boiler inlet ($p_{BFW}$), at medium pressure turbine inlet ($p_{RH}$) and in the condenser ($p_{cond}$). It is recalled that the SH outlet pressure is constant thanks to the partial arc admission control. The boiler feed water pressure slightly decreases in the *Baseline* case because of the reduction of the pressure drops with reduced steam flow rate. In the *FlexiCaL* case, the water flow rate and pressure drop in the calciner line heat exchanger remains almost constant at part-load due to the constant heat input and equivalent pressure drops must be ensured through throttling in the carbonator and sorbent cooling lines to maintain a proper split ratio of the water in the different parallel lines. Reheating pressure reduces because of the reduction of RH steam mass flow rate and the sliding pressure control of the medium pressure turbine. Condensation pressure also reduces because of the lower heat duty at part-load and the assumed constant cooling water flow rate. Reheating pressure and condensation pressure reduction are less marked in the *FlexiCaL* case than in the *Baseline* case because of the lower reduction of the heat recovered by the steam cycle and of the steam flow rate (Fig. 5 right).
- Fig. 8 depicts the variation of the heat share of the CaL unit heat exchangers vs. the PCPP load. Fig. 9 depicts the temperature-heat diagrams of the main water heating lines (the carbonator, the calciner and the sorbent cooling lines) for the *FlexiCaL* case at nominal and minimum load (left and right columns respectively). As shown in Fig. 8.a and Fig. 8.b for the *Baseline* case and *FlexiCaL* case respectively, the reduction of the available thermal power from the carbonator line leads to a different share of the heat extracted from the reactor riser waterwalls and the heat extracted from the carbonator external heat exchangers. The duty of the different carbonator line sections and their variation with respect to the design load are substantially the same in both the *Baseline* and *FlexiCaL* cases, because the carbonator island is always designed on the nominal PCPP flue gas mass flow rate and operated following PCPP load. Heat transferred in the carbonator riser ($Q_{1.a,SH2}$) slightly reduces when

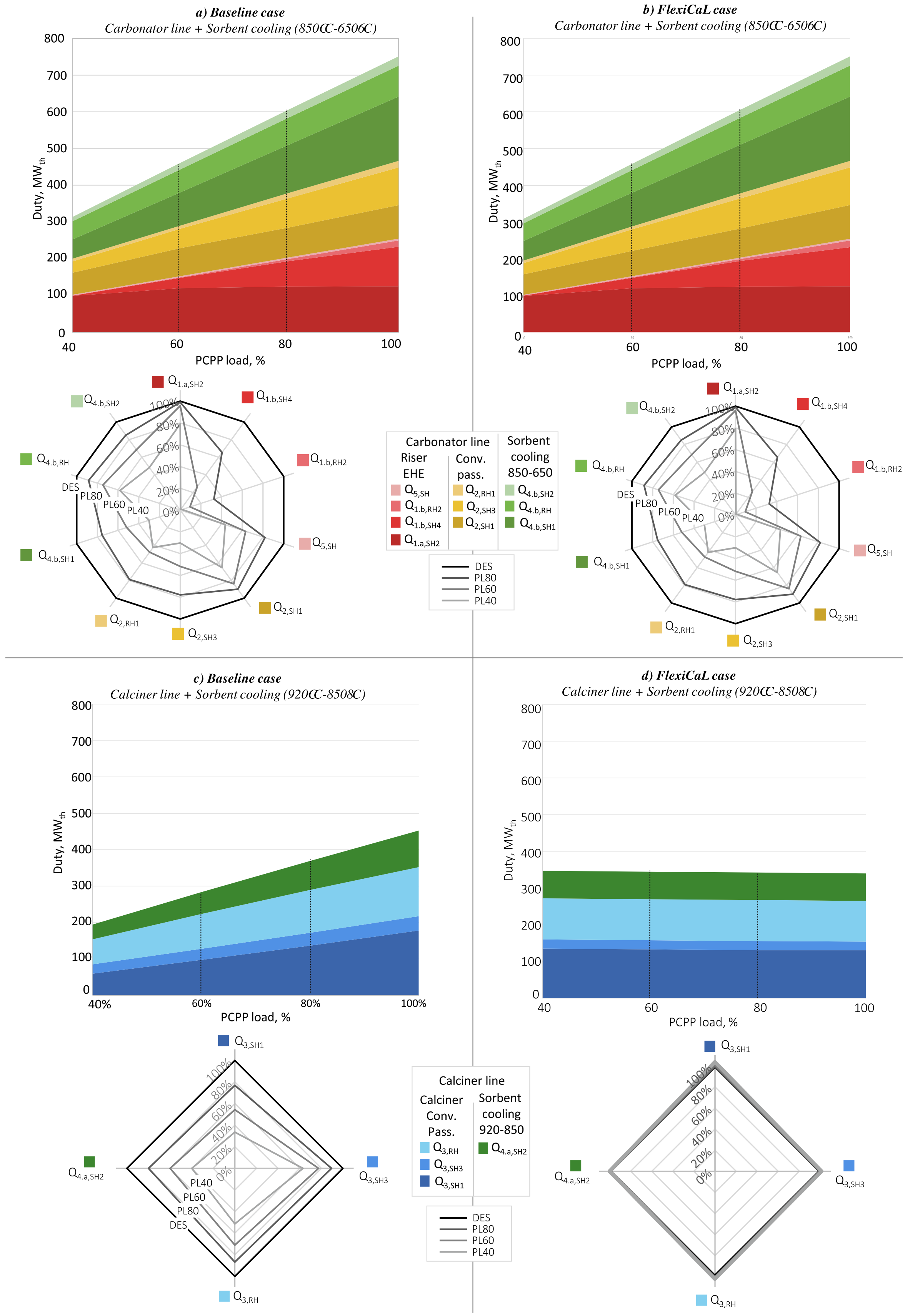


**Fig. 8.** Part-load behaviour of different sections of the high temperature SH and RH lines. Carbonator and low temperature sorbent cooling lines of *Baseline* (a) and *FlexiCaL* cases (b); calciner and high temperature sorbent cooling lines of *Baseline* case (c) and of *FlexiCaL* case (d). The radar plots show the duty variation with respect to the design load; plots show the absolute change of duty.

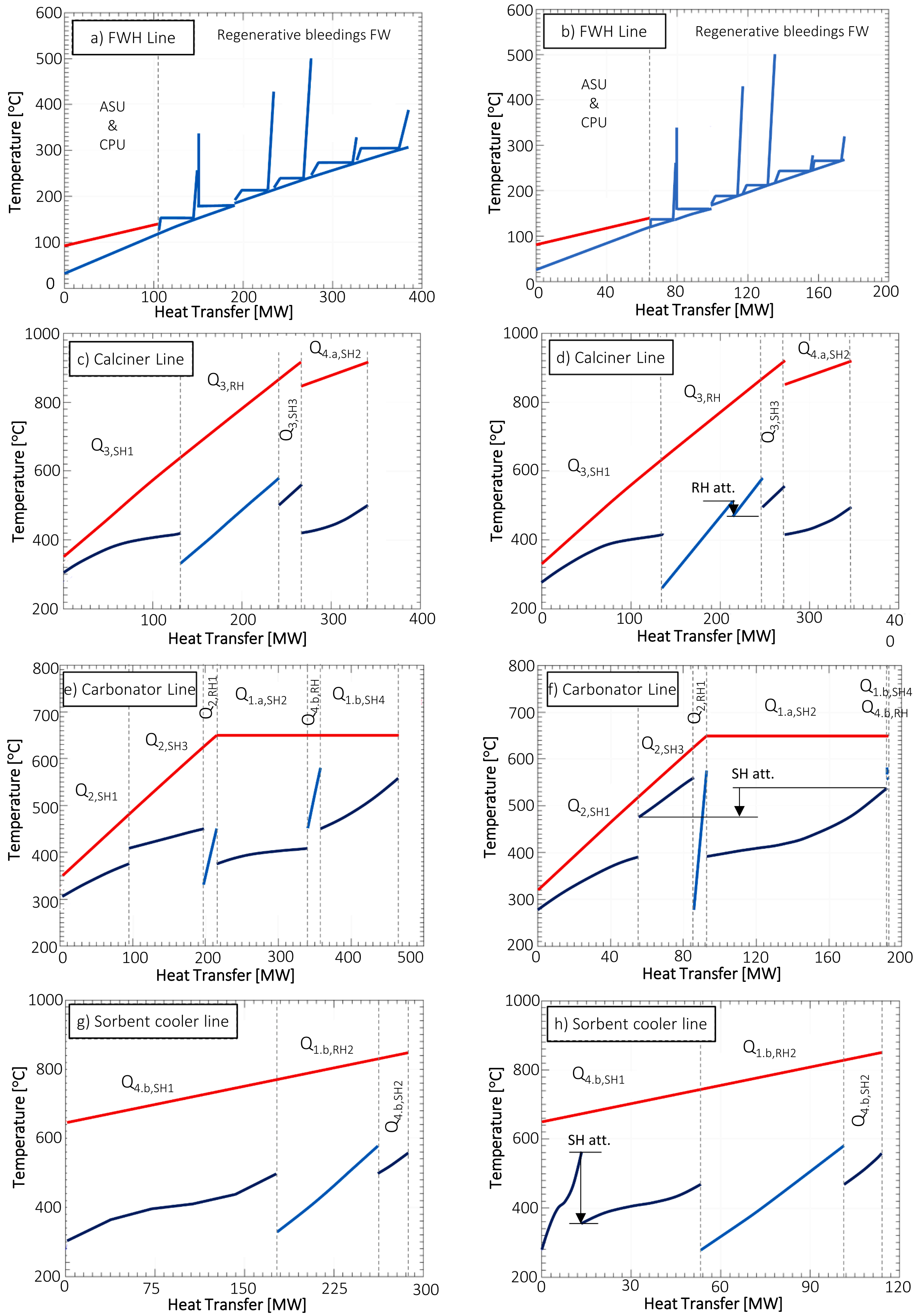


**Fig. 9.** Temperature-heat diagrams of feedwater preheating, calciner, carbonator and sorbent cooling lines for the *FlexiCaL* case with the PCPP at 100% load (left) and 40% load (right). Arrows show the main steam attemperation.

reducing the PCPP load because of the constant overall heat transfer coefficient in the waterwalls tubes and the increase of the average water temperature. As shown in Fig. 9.f, both the inlet and outlet water temperature in the carbonator waterwalls increase when PCPP load reduces and significant attemperation is required at low PCPP loads after the $Q_{1.a,SH2}$ exchanger. At 40% load, steam superheating ($Q_{2,SH3}$) and reheating ($Q_{2,RH1}$) are completed in the convective pass (Fig. 9.f) and both external heat exchangers are closed ($Q_{1.b,SH4}$ and $Q_{4.b,RH}$). As a result, in the carbonator line the share of heat dedicated to live steam production increases with respect to the heat available for steam reheating, leading to a modifications also in the heat share in the calciner (Fig. 9.d) and hot sorbent cooling lines (Fig. 9.h). RH/SH steam ratio increases in both these lines and attemperation is mainly required in the calciner line RH and in the first SH in the sorbent cooler line.

- The main difference between the *Baseline* and the *FlexiCaL* cases is the variation of the thermal power transferred in the calciner and high temperature sorbent cooling lines. While in the *Baseline* case, it roughly follows the PCPP load (Fig. 8.c), in the *FlexiCaL* case it is substantially independent of the PCPP load (Fig. 8.d).
- In the DES-HIGH case, the flow rate of solids through the sorbent cooling line is increased by 30% compared to the nominal case leading to an increase of around 20% of the high pressure steam flow rate in this path and an increase of pressure drop (+22 bar) with respect to the nominal operation. The temperature of the solids at the exit of this cooling section increases from 650 °C to 668 °C. The steam flow rate in the remaining two lines of the system remains unchanged and equal to the nominal case value. The higher steam flow rate produced in CaLPP leads to a higher reheating pressure which causes a different distribution of the steam flow rate in the various reheating lines. Steam flow rate through the reheater bundles increases by 21% in the sorbent cooling line, it decreases by about 8% in the calciner line and remains unchanged in the carbonator compared to the nominal operating point.
- In the PL40-LOW case, the fluidization of the sorbent cooling line is interrupted and no solids are extracted from the high temperature vessel of primary storage. In this case the live steam produced in the CaLPP decreases by about 18% compared to the PL40 case. The superheated steam parameters at the HP turbine inlet are substantially equal to the PL40 operating point. On the other hand, the closure of the sorbent cooling line causes a slight reduction of the reheated steam temperature (570 °C vs 580 °C) because of the higher steam flow rate in the reheating line of the calciner (about 21% more) and the reduction of the cold reheat temperature caused by the reduction of IP turbine inlet pressure.

### 4.3. Power balance

The performance comparison between the *Baseline* and *FlexiCaL* cases is carried out on two main figures for weekday operation: the

**Table 10**
*Baseline* case part-load power balance.

| *Baseline case* | DES | PL80 | PL60 | PL40 |
|---|---|---|---|---|
| *PCPP* | | | | |
| Relative flue gas flow rate, % | 100.0 | 80.0 | 60.0 | 40.0 |
| Net power output, MW | 747.2 | 593.3 | 438.1 | 280.6 |
| Coal input, kg/s | 66.61 | 53.29 | 39.96 | 26.64 |
| Coal thermal input, $MW_{LHV}$ | 1676.5 | 1341.2 | 1005.9 | 670.6 |
| Net electric efficiency, $\%_{LHV}$ | 44.57 | 44.14 | 43.28 | 41.25 |
| *CaLPP - Electric Power Balance, MW* | | | | |
| Steam turbine | 641.7 | 520.5 | 392.7 | 262.1 |
| Boiler feed water pump | −25.05 | −18.86 | −14.35 | −11.10 |
| Condensate extraction pump | −0.79 | −0.50 | −0.31 | −0.18 |
| Condenser auxiliaries | −9.05 | −9.11 | −9.17 | −9.24 |
| Auxiliaries for heat rejection (other than cond.) | −0.71 | −0.56 | −0.42 | −0.27 |
| Coal milling and handling | −2.53 | −2.02 | −1.52 | −1.01 |
| Filters and ash handling* / Purge and limestone handling** | −4.78 | −3.82 | −2.87 | −1.91 |
| Primary air FD fan* / Carbonator FD fan** | −11.97 | −9.57 | −7.18 | −4.79 |
| Secondary air FD fan/$CO_2$ recirculation fan | −5.36 | −4.29 | −3.22 | −2.15 |
| Boiler ID fan* / Carbonator ID fan** | −2.83 | −2.27 | −1.70 | −1.13 |
| ASU | −70.61 | −56.49 | −42.37 | −28.24 |
| CPU | −122.10 | −97.68 | −73.26 | −48.84 |
| BOP | −9.80 | −8.18 | −6.50 | −4.78 |
| Net electric power output, MW | 376.1 | 307.2 | 229.9 | 148.5 |
| Coal input, kg/s | 53.92 | 43.14 | 32.35 | 21.57 |
| Coal thermal input, $MW_{LHV}$ | 1357.2 | 1085.8 | 814.3 | 542.9 |
| Net electric efficiency, $\%_{LHV}$ | 27.71 | 28.29 | 28.23 | 27.35 |
| $\eta_{QHT}$, % | 50.42 | 50.39 | 49.53 | 47.57 |
| *PCPP & Baseline CaLPP* | | | | |
| Net power output, MW | 1123.3 | 900.5 | 668.0 | 429.1 |
| Relative net power output, % | 100 | 80.16 | 59.46 | 38.20 |
| Coal input, kg/s | 120.53 | 96.42 | 72.32 | 48.21 |
| Coal thermal input, $MW_{LHV}$ | 3033.7 | 2427.0 | 1820.2 | 1213.5 |
| Net electric efficiency, $\%_{LHV}$ | 37.03 | 37.10 | 36.70 | 35.36 |
| Efficiency penalty with respect to PCPP, %pts. | −7.54 | −7.13 | −6.85 | −6.49 |
| Direct $CO_2$ emission at stack, kg/s | 16.23 | 12.99 | 9.74 | 6.49 |
| $CO_2$ vented from the CPU, kg/s | 8.77 | 7.02 | 5.26 | 3.51 |
| Specific emissions, $kg_{CO2}$/MWh | 80.1 | 80.0 | 80.8 | 83.9 |
| SPECCA, $MJ_{LHV}/kgCO_2$ | 2.34 | 2.21 | 2.14 | 2.11 |

* Items referred to the PCPP plant.
** Items referred to the *Baseline* and *FlexiCaL* CaL plants.

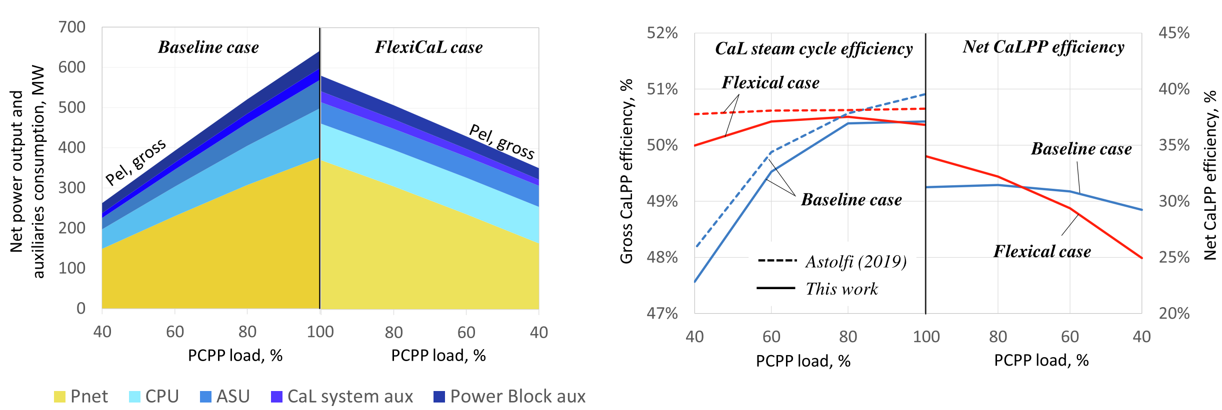


**Fig. 10.** (left) power output and auxiliary consumption; (right) CaL steam cycle and net CaLPP efficiencies vs. PCPP load. Steam cycle efficiency curves are derived by combining Figs. 6 and 7 available in Astolfi et al. (2019) [33].

**Table 11**
*FlexiCaL* case part-load power balance.

| *FlexiCaL case* | DES | PL80 | PL60 | PL40 | WE-MIN | DES-HIGH | PL40-LOW |
|---|---|---|---|---|---|---|---|
| *PCPP* | | | | | | | |
| Relative flue gas flow rate, % | 100.0 | 80.0 | 60.0 | 40.0 | 40.0 | 100.0 | 40.0 |
| Net power output, MW | 747.2 | 593.3 | 438.1 | 280.6 | 280.6 | 747.2 | 280.6 |
| Coal input, kg/s | 66.61 | 53.29 | 39.96 | 26.64 | 26.64 | 66.61 | 26.64 |
| Coal thermal input, $MW_{LHV}$ | 1676.5 | 1341.2 | 1005.9 | 670.6 | 670.6 | 1676.5 | 670.6 |
| Net electric efficiency, $\%_{LHV}$ | 44.57 | 44.14 | 43.28 | 41.25 | 41.25 | 44.57 | 41.25 |
| *CaL + CaLPP - Electric Power Balance, MW* | | | | | | | |
| Steam turbine | 580.7 | 507.0 | 430.2 | 350.5 | 261.7 | 603.8 | 292.1 |
| Boiler feed water pump | −22.73 | −19.33 | −16.50 | −14.19 | −11.68 | −25.85 | −12.68 |
| Condensate extraction pump | −0.68 | −0.53 | −0.40 | −0.30 | −0.19 | −0.72 | −0.24 |
| Condenser auxiliaries | −8.20 | −8.23 | −8.27 | −8.30 | −8.36 | −8.19 | −8.34 |
| Auxiliaries for heat rejection (other than cond.) | −0.53 | −0.53 | −0.53 | −0.53 | −0.28 | −0.53 | −0.53 |
| Coal milling and handling | −1.90 | −1.90 | −1.90 | −1.90 | −1.01 | −1.90 | −1.90 |
| Filters and ash handling* / Purge and limestone handling** | −4.78 | −3.82 | −2.87 | −1.91 | −1.91 | −4.78 | −1.91 |
| Primary air FD fan* / Carbonator FD fan** | −11.97 | −9.57 | −7.18 | −4.79 | −4.79 | −11.97 | −4.79 |
| Secondary air FD fan* / $CO_2$ recirculation fan** | −4.02 | −4.02 | −4.02 | −4.02 | −2.15 | −4.02 | −4.02 |
| Boiler ID fan* / Carbonator ID fan** | −2.83 | −2.27 | −1.70 | −1.13 | −1.13 | −2.83 | −1.13 |
| ASU | −52.96 | −52.96 | −52.96 | −52.96 | −28.24 | −52.96 | −52.96 |
| CPU | −91.58 | −91.58 | −91.58 | −91.58 | −48.84 | −91.58 | −91.58 |
| BOP | −8.55 | −7.82 | −7.05 | −6.25 | −4.65 | −8.78 | −5.67 |
| Net electric power output, MW | 370.0 | 304.5 | 235.3 | 162.6 | 148.5 | 390.5 | 107.2 |
| Coal input, kg/s | 40.44 | 40.44 | 40.44 | 40.44 | 21.57 | 40.44 | 40.44 |
| Coal thermal input, $MW_{LHV}$ | 1017.9 | 1017.9 | 1017.9 | 1017.9 | 542.9 | 1017.9 | 1017.9 |
| $\eta_{QHT}$, % | 50.36 | 50.51 | 50.43 | 50.00 | 47.87 | 49.94 | 49.84 |
| *PCPP & FlexiCaL CaLPP* | | | | | | | |
| Net power output, MW | 1117.2 | 897.8 | 673.3 | 443.2 | 429.1 | 1136.9 | 387.0 |
| Relative net power output, % | 100.0% | 80.4% | 60.3% | 39.7% | 38.4% | 101.8% | 34.6% |
| Coal input, kg/s | 107.05 | 93.73 | 80.40 | 67.08 | 48.21 | 107.05 | 67.08 |
| Coal thermal input, $MW_{LHV}$ | 2694.4 | 2359.1 | 2023.8 | 1688.5 | 1213.5 | 2694.4 | 1688.5 |
| Direct $CO_2$ emission at stack, kg/s | 16.23 | 12.99 | 9.74 | 6.49 | 6.49 | 16.23 | 6.49 |
| $CO_2$ vented from the CPU, kg/s | 6.58 | 6.58 | 6.58 | 6.58 | 3.51 | 6.58 | 6.58 |

* Items referred to the PCPP plant.
** Items referred to the Baseline and FlexiCaL CaL plants.

power output and the efficiency of the CaLPP. The following observations can be made:

- CaLPP gross and net power output decrease almost linearly with the PCPP load (Fig. 10.left) in both *Baseline* and *FlexiCaL* cases. Both quantities are slightly higher for the *Baseline* case in nominal condition while they are higher for the *FlexiCaL* case at minimum load.
- CaL steam cycle efficiency can be calculated as the steam cycle net power output (generator gross power minus power block auxiliaries like pumps and condenser auxiliaries) divided by the heat input at high temperature (eq. (1)).

$$\eta_{QHT} = \frac{\dot{W}_{CaL\ SC}}{\sum_{i=0}^{5} Q_i} = \frac{\dot{W}_{turbine} - \dot{W}_{pumps} - \dot{W}_{condenser\ aux}}{Q_{tot} - Q_6 - Q_{ASU} - Q_{CPU}} \quad (1)$$

This quantity is meaningful also for the *FlexiCaL* case even in operating points where solids in the storage silos are being used, since it refers to the steam cycle heat input and not to the fuel input. The CaL steam cycle efficiency decreases at low PCPP loads (Fig. 10.right) because of:

- the reduction of the boiler feedwater temperature ($T_{BFW}$), caused by the reduction of the steam bleeding pressure (see Fig. 9.b);
- the reduction of the turbine efficiency: the main penalty is for the first group of stages of the high pressure turbine because of the reduction of degree of admission, while efficiency of the low pressure turbine slightly increases at part-load thanks to the higher vapor fraction at turbine outlet and the lower kinetic losses of the exhaust steam;
- the need of attemperation in the reheaters at part-load (while attemperation of superheaters does not involve any efficiency decay).

The first two effects penalize the *Baseline* case by a larger extent, as it is subject to a higher reduction of SH and RH steam mass flow rates, while the opposite happens with the third effect.

In Fig. 10.right, the CaL steam cycle efficiency is compared with the correlation used in the previous publication [33], derived from literature data on conventional steam power plants. This figure shows a good agreement between the correlation and the values found in this work, with differences within 0.5 percentage points at all loads.

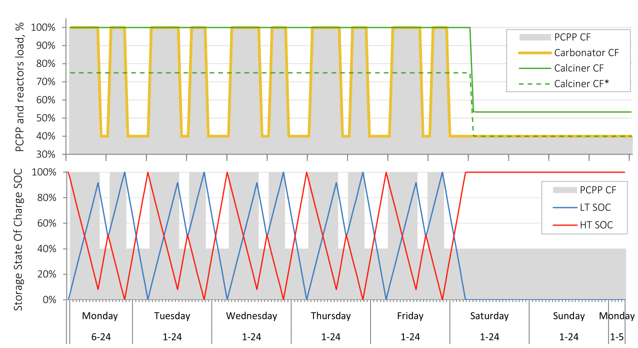


**Fig. 11.** (top) trend of hourly capacity factor of PCPP, carbonator and calciner reactors for one week of operation for the *FlexiCaL* case. Calciner CF* is calculated with reference to the nominal calciner load of the *Baseline* case. (Bottom) State of Charge (SOC) of high temperature and low temperature tanks of the primary storage system.

Finally, Fig. 10.right depicts the net CaLPP efficiency calculated considering also the consumption of ASU and CPU compressors. This index is higher at PCPP full load for the *FlexiCaL* case thanks to the smaller calciner line, while it is lower at minimum PCPP load because the ASU and CPU compressor consumption is constant rather than decreasing with the PCPP load as in *Baseline* case.

Tables 10 and 11 show the power balance of the assessed systems at different operating conditions according to the grid of Table 6. In the *Baseline* case, the net electric efficiency penalty compared to the PCPP reduces from 7.5 percentage points at full load to 6.5 points at minimum load. This is motivated by the different part-load penalization for the PCPP and CaLPP at low loads. The PCPP stack temperature is kept constant in order to avoid acid gas condensation. On the other hand, the boiler efficiency of the CaLPP increases by 3% at the minimum load thanks to the higher heat exchanger effectiveness that allows to reduce the convective pass outlet temperature and increase the recovery of $CO_2$ sensible heat. As a result, the CaLPP efficiency is slightly dependent on the load. The specific $CO_2$ emission increases at low loads due to the lower efficiency of complete PCPP & CaLPP system. All these aspects affect the value of SPECCA, which decreases from 2.34 MJ/kg$_{CO2}$ at design point to 2.11 MJ/kg$_{CO2}$ at the minimum load.

For the *FlexiCaL* case, the balance of three additional cases is reported in Table 11:

- The WE-MIN operating point represents the operating conditions at minimum load during the week-end, when the high temperature sorbent storage is fully charged and the plant is required to operate at the minimum load. In this condition, the calciner island must also reduce the load, resulting in operating parameters and overall energy balance very similar to the *Baseline* PL40-case.
- The DES-HIGH operating point represents the case where the secondary storage is exploited to provide extra power output, above the nominal power output. With the assumed solids flow rate increase of 30%, the electric power output of the whole plant increases by 20 MW$_e$, i.e. by 1.8% if referred to the overall system power output and by 5.5% if referred to the sole CaLPP.
- The PL40-LOW operating point represents the case where the secondary storage is exploited to reduce the overall power output, below the minimum load. By interrupting the flow of solids through the sorbent cooler, the power output can be reduced by 56.2 MW, i.e. by 12.7% if referred to the overall system power output and by 34.6% if referred to the sole CaLPP.

### 4.4. Cyclic energy balance

An additional set of results refers to cyclic energy balances on daily base for both week days, weekend days and overall weekly operation. Fig. 11 depicts the weekly capacity factor for PCPP, carbonator and calciner reactors plus the state of charge (SOC) of the high temperature and low temperature tanks of the primary storage system of the *FlexiCaL* case. The PCPP capacity factor (CF) is calculated with respect to the nominal coal consumption and also refers to flue gas mass flow rate (see Table 3). The carbonator always follows the PCPP load. The calciner, thanks to the availability of primary storage always works in nominal condition during the weekdays (CF = 100%) and at minimum load in the weekend, when the high temperature primary storage tank is full.

Results are presented for the PCPP in Table 12 while Table 13 shows the cyclic results for the *Baseline* and *FlexiCaL* cases. Daily quantities are meaningful also for the *FlexiCaL* case thanks to the choice of designing the calciner island on the weekday average PCPP flue gas mass flow rate capacity factor. The following observations can be made:

- CaLPP system shows a slightly higher efficiency in the *FlexiCaL* case than in the *Baseline* case on the weekday cyclic operation, thanks to the lower part-load penalization due to a less variable thermal input and the lower part-load efficiency decay of the steam cycle.
- Differences between *Baseline* and *FlexiCaL* cases is negligible for the weekend day, since the performance of the two systems is very similar (see column PL40 of Table 10 and column WE-MIN of Table 11 for *Baseline* and *FlexiCaL* cases respectively).
- The weekly cyclic operation favours the *FlexiCaL* case thanks to a slightly lower efficiency penalty resulting in a slightly lower SPECCA value. On the contrary, $CO_2$ emissions are equal between the two cases since carbonator capture efficiency is never limited in the *FlexiCaL* case and the overall fuel required in the calciner is the same. On the whole, the overall performances of *Baseline* and *FlexiCaL* cases are very similar because during the weekday operation the number of full load hours (where *FlexiCaL* case efficiency is higher than the *Baseline* case) is similar to the number of minimum load hours (where *FlexiCaL* case efficiency is lower than the *Baseline* case as reported in Fig. 10.right).

**Table 12**
Energy balance of the PCPP for weekday, weekend day and overall week operation.

| PCPP | Weekday | Weekend day | Week |
|---|---|---|---|
| Steam cycle gross energy output, MWh | 13,708 | 6970 | 82,479 |
| Auxiliary consumption, MWh | 335.7 | 179.0 | 2036.6 |
| FGD, MWh | 59.9 | 31.9 | 363.4 |
| BOP, MWh | 45.3 | 24.1 | 274.6 |
| Net electric energy output, MW | 13,267 | 6734 | 79,804 |
| Capacity Factor | 74.0% | 37.6% | 63.6% |
| Fuel input, MWh$_{LHV}$ | 30,177 | 16,094 | 183,074 |
| Net electric efficiency, %$_{LHV}$ | 44.0% | 41.8% | 43.6% |
| Coal consumption, ton | 4316 | 2302 | 26,185 |
| Flue gases mass flow rate, ton | 48,198 | 25,706 | 292,403 |
| Emitted $CO_2$, ton | 10,527 | 5615 | 63,866 |
| Specific emission, kg/MWh | 793.5 | 833.7 | 800.3 |

### 4.5. Economic analysis

The final analysis focuses on the economic evaluation of the capital investment cost of the *Baseline* and *FlexiCaL* cases and the calculation of the Levelized Cost of Electricity (LCOE) for both cases.

Table 14 reports the capital cost breakdown for PCPP, *Baseline* and *FlexiCaL* cases adopting the set of cost correlations presented in [33]. The incremental capital cost of the *Baseline* and *FlexiCaL* cases with respect to the PCPP installation is remarkable, as the total capital cost (in M€) roughly doubles with the CaLPP section. On the other hand, the additional power output of the CaL plants results in a lower increment of the specific cost (in €/kW), that increases by 42% in the *Baseline* case and by 34% in the *FlexiCaL* case. The highest cost components in the PCPP are the boiler and the power block representing 37% and 32% of the equipment cost (i.e. excluding electrical, instrumentation and control, improvement to site, buildings and structures and TASC + owner's costs). For the CaLPP section of the *Baseline* case, the largest shares are associated to the power block (20%), the ASU (18.4%), the carbonator reactor and convective pass (13.7%), the CPU (11%), the sorbent heat exchangers (10.7%) and the calciner reactor and convective pass (9.1%), highlighting once again the potential attainable by reducing calciner island components size.

The calculation of the LCOE is based on a set of fixed assumptions on coal (65 €/t) and limestone (15 €/t) specific cost, fixed (0.0258€/TASC – year) and variable (3.83 €/MWh) Opex, $CO_2$ transport and storage cost (7 €/t), in line with [46,47], and Carrying Charge Factor (CCF) (0.11) for investment cost annualization [33]. LCOE results are reported in Table 15 for a carbon tax of 50 €/ton (close to the breakeven value with the *Baseline* CaL case) and a plant availability of 90% on annual basis.

With respect to the PCPP, both *Baseline* and *FlexiCaL* cases show a higher LCOE share for all the cost components but the $CO_2$ emission cost. The higher capital cost, the higher coal and limestone consumption, the higher variable and fixed Opex are compensated by the savings related to carbon tax, resulting in a LCOE of *Baseline* and *FlexiCaL* cases lower

**Table 13**
Energy balance of the CaLPP section and overall system (PCPP + CaLPP) for weekday, weekend day and overall week operation for the *Baseline* and *FlexiCaL* cases. Capacity factor is referred to the net electric energy produced in 24 h of continuous operation at nominal (DES) power output.

| | Baseline case | | | FlexiCaL case | | |
|---|---|---|---|---|---|---|
| CaLPP | Weekday | Weekend day | Week | Weekday | Weekend day | Week |
| Steam turbine generator output, MWh | 11604.5 | 6290.4 | 70603.1 | 11634.4 | 6280.6 | 70733.2 |
| Steam cycle auxiliaries, MWh | −693.8 | −492.6 | −4454.0 | −670.4 | −485.5 | −4322.8 |
| CaL auxiliaries, MWh | −507.1 | −270.1 | −3075.6 | −507.2 | −270.5 | −3077.2 |
| ASU, MWh | −1271.0 | −677.9 | −7710.9 | −1271.0 | −677.9 | −7710.9 |
| CPU, MWh | −2197.8 | −1172.2 | −13333.3 | −2197.8 | −1172.2 | −13333.3 |
| BOP, MWh | −185.0 | −114.8 | −1154.7 | −182.3 | −111.6 | −1134.6 |
| Net electric energy output, MWh | 6749.8 | 3562.8 | 40874.4 | 6805.7 | 3562.9 | 41154.4 |
| CaL coal consumption, t | 3494.1 | 1863.6 | 21197.7 | 3494.1 | 1863.5 | 21197.4 |
| Fuel input, $MWh_{LHV}$ | 24,429 | 13,029 | 148,206 | 24,429 | 13,029 | 148,205 |
| Net electric efficiency, $\%_{LHV}$ | 27.6% | 27.3% | 27.6% | 27.9% | 27.3% | 27.8% |
| Overall system (PCPP & CaLPP) | Weekday | Weekend day | Week | Weekday | Weekend day | Week |
| Net electric energy output, MWh | 20,017 | 10,297 | 120,678 | 20,073 | 10,297 | 120,958 |
| Capacity Factor | 74.2% | 38.2% | 63.9% | 74.5% | 38.4% | 64.4% |
| Coal consumption, ton | 7810 | 4165 | 47,382 | 7810 | 4165 | 47,382 |
| Fuel input, $MWh_{LHV}$ | 54,606 | 29,123 | 331,279 | 54,606 | 29,123 | 331,279 |
| Net electric efficiency, $\%_{LHV}$ | 36.7% | 35.4% | 36.4% | 36.8% | 35.4% | 36.5% |
| Efficiency penalty with respect to PCPP, %pts. | −7.31 | −6.49 | −7.16 | −7.21 | −6.49 | −7.08 |
| Direct $CO_2$ emission at stack, t | 1051.9 | 561.0 | 6381.3 | 1051.9 | 561.0 | 6381.3 |
| $CO_2$ vented from the CPU, t | 568.2 | 303.1 | 3447.3 | 568.2 | 303.1 | 3447.3 |
| Specific emission, kg/MWh | 80.94 | 83.91 | 81.44 | 80.71 | 83.91 | 81.26 |
| SPECCA, $MJ_{LHV}/kg_{CO2}$ | 2.29 | 2.11 | 2.26 | 2.25 | 2.10 | 2.23 |

**Table 14**
Capital cost breakdown for PCPP and for both *Baseline* and *FlexiCaL* cases.

| Capital cost [M€] | PCPP | Baseline | FlexiCaL |
|---|---|---|---|
| Power block (Steam turbine, generator, condenser, feedwater) | 303.27 | 560.18 | 543.07 |
| PC boiler (coal handling excluded) | 350.27 | 350.27 | 350.27 |
| Ducting & Stack | 43.83 | 40.11 | 40.11 |
| Carbonator reactor | – | 88.18 | 88.18 |
| Carbonator conv pass | – | 89.45 | 89.45 |
| Calciner reactor (coal handling excluded) | – | 19.55 | 14.75 |
| Calciner conv pass | – | 97.43 | 76.30 |
| Coal handling, crushing, drying | 46.01 | 66.85 | 62.04 |
| Ash handling | 19.46 | 41.86 | 37.30 |
| Sorbent handling, crushing, drying | 3.52 | 35.84 | 29.98 |
| Solids heat exchanger HT | – | 35.77 | 26.97 |
| Solids heat exchanger LT + purge | – | 102.11 | 102.11 |
| ASU | – | 236.89 | 199.34 |
| CPU | – | 144.53 | 120.76 |
| Flue gas clean up (FGD excluded) | 41.48 | 34.95 | 34.95 |
| FGD | 131.97 | 131.97 | 131.97 |
| Solids storage | – | – | 9.69 |
| Electrical equipment | 60.44 | 126.80 | 117.06 |
| Instrumentation and control | 21.00 | 26.27 | 25.64 |
| Improvement to site | 13.16 | 15.38 | 15.20 |
| Buildings & Structures | 51.38 | 55.78 | 55.43 |
| TASC + owner's | 417.03 | 883.45 | 833.67 |
| Total capital expenditure, M€ | 1502.8 | 3183.6 | 3004.2 |
| Specific cost, €/kW | 2011 | 2850 | 2689 |

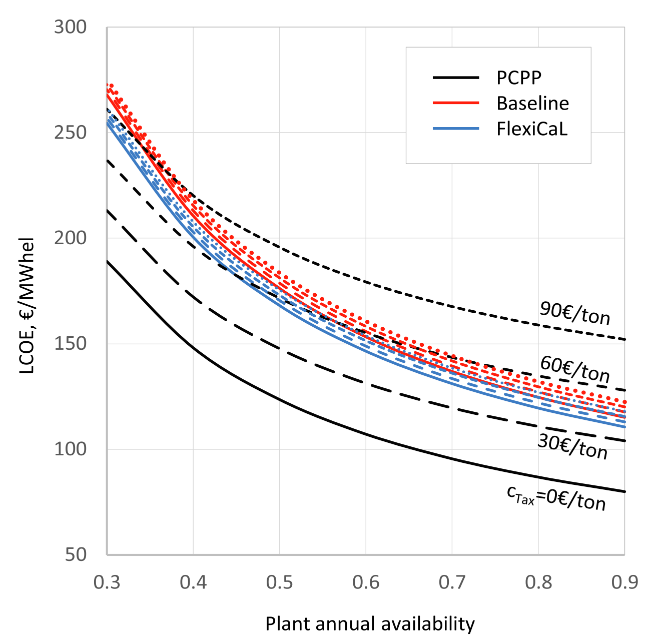


**Fig. 12.** Sensitivity analysis on the LCOE as function of the plant annual availability and the carbon tax value for the PCPP, the *Baseline* and the *FlexiCaL* cases.

**Table 15**
LCOE breakdown for PCPP, *Baseline* and *FlexiCaL* cases for a carbon tax of 50 €/ton and plant availability of 90%.

| LCOE breakdown [€/MWh] | PCPP | Baseline | FlexiCaL |
|---|---|---|---|
| Capex | 44.14 | 61.84 | 58.22 |
| Coal | 21.33 | 25.52 | 25.46 |
| Limestone | 0.07 | 1.86 | 1.85 |
| Fixed Opex | 10.35 | 14.50 | 13.65 |
| Variable Opex | 4.13 | 4.97 | 4.96 |
| $CO_2$ transport and storage | 0.00 | 6.47 | 6.45 |
| $CO_2$ emission | 40.01 | 4.07 | 4.06 |
| LCOE | 120.04 | 119.23 | 114.66 |

than the PCPP. The *FlexiCaL* case is the one with the lowest LCOE, about 4.4% less than the PCPP and the *Baseline* CaL cases. Compared to the *Baseline* case, the economic benefit of the *FlexiCaL* case is related to the lower Capex and fixed Opex (computed as a fraction of the Capex).

Finally, Fig. 12 depicts a sensitivity analysis varying both the carbon tax value (0 €/ton, 30 €/ton, 60 €/ton, 90 €/ton) and the plant availability between 30% and 90%. Results show that the *FlexiCaL* storage always allows to reduce the LCOE by around 4–5% with respect to the *Baseline* case, independently of the value of the carbon tax and the plant availability. The two CaL cases may also be compared on the breakeven capacity factor, considering that the adoption of a $CO_2$ capture technology is profitable only if the plant availability is sufficiently high to pay back the additional capital cost. The minimum plant availability that makes the *FlexiCaL* and *Baseline* cases economically competitive with the PCPP reduces as the carbon tax increases. For a carbon tax of 60 €/ton, the minimum availability is 52% for the *FlexiCaL* case and 66% for the *Baseline* case. For a carbon tax of 90 €/ton, the minimum availability reduces to 30% for the *FlexiCaL* case and to 38% for the *Baseline* case.

It has to be highlighted that the obtained quantitative results cannot be extended to cases with a power production profile different from the one assumed in this study. So, the calculations at different capacity factors consider the operation of the plant with the same weekly production profile but for a lower number of weeks per year. Also, the LCOE indicator of the *FlexiCaL* is not suitable to evaluate the benefit of the secondary storage system for the operation on the balancing market, for which a different approach is needed in the economic analysis.

## 5. Conclusions

In this work, a comprehensive techno-economic analysis of CaL plants without and with sorbent storage systems has been carried out, with accurate modelling of the part-load performance resulting from weekly cycling operations. The analysis carried out in this work allows to compare three plants, namely: (i) a conventional ultra supercritical pulverized coal power plant (PCPP) without $CO_2$ capture, (ii) a *Baseline* CaL plant for $CO_2$ capture from the PCPP plant flue gas and (iii) a *FlexiCaL* Calcium looping plant integrating a primary sorbent storage system to decouple the carbonator and the calciner load and reduce the size of the calciner island and a secondary sorbent storage to increase/reduce the maximum/minimum power output of the plant for improved grid services. Heat and mass balances have been computed for the CaL plants at different loads, taking into account the off-design performance of heat exchangers and machines. A simplified economic analysis has been carried out to compute the cost of electricity and estimate the economic benefits of the primary sorbent storage system for a given power generation profile.

The following main conclusions can be listed from the results of this work:

- In CaL plants designed for flexible operations, the carbonator reactor should be designed with heat transfer surface mainly placed in external heat exchangers, outside the riser. As a matter of fact, since the heat transfer coefficient in a CFB riser is slightly affected by the load, high heat transfer surface area would involve excessive cooling of the carbonator bed at low load, with consequent reduction of energy efficiency and sorbent performance. On the other hand, heat transfer rate in the external heat exchangers can be controlled more easily by adjusting the bed fluidization and operating on a solids bypass. In this work, the carbonator has been designed with a relative low height of 20 m, sufficient to achieve the target $CO_2$ capture rate and to accommodate the CFB cyclones, and with no additional heat transfer surface inside the riser apart from the membrane waterwalls.
- Thanks to the constant heat input from the calciner island that operates with the design fuel input also when the PCPP and carbonator load are reduced, the steam cycle of the *FlexiCaL* case receives a more stable heat input, resulting in a higher part-load efficiency than the *Baseline* CaL case. However, with the assumed production profile, the electric efficiency computed on a weekly basis is not significantly affected (about 0.1% point of efficiency difference).
- The adoption of a secondary storage allows increased operativity of the *FlexiCaL* plant on the balancing market, with variation of +2% (i.e. + 20 $MW_e$ for the assumed plant size) power output compared to the nominal load and −13% (i.e. −56 $MW_e$) power output compared to the minimum load.
- With the assumed production profile, the *FlexiCaL* primary storage allows to reduce the cost of electricity by around 4–5% with respect to the *Baseline* case, independently of the value of the carbon tax and of the plant availability.

## Declaration of Competing Interest

The authors declare that they have no known competing financial interests or personal relationships that could have appeared to influence the work reported in this paper.

## Acknowledgements

The project “FlexiCaL” leading to this study has received funding from the Research Fund for Coal and Steel under grant agreement No 709629.

## Appendix A. Supplementary material

Electronic Supplementary Information (ESI) available: here are reported the tables related to the streams shown in Figs. 1 and 2 and the tables with the sizing of the various components for the *Baseline* case. Supplementary data to this article can be found online at https://doi.org/10.1016/j.applthermaleng.2021.117048.

## References

[1] IEA, Composition of CO2 emissions and emission intensity in 2020, IEA, Paris, 2020. Available from: <https://www.iea.org/data-and-statistics/charts/composition-of-co2-emissions-and-emission-intensity-in-2020>.
[2] IEA, World Energy Outlook 2019, World Energy Outlook 2019, 2019, 807.
[3] IEA, Special Report on Carbon Capture Utilisation and Storage, 2020.
[4] OECD/IEA, World Energy Outlook 2018: Electricity, 2018.
[5] R. Domenichini, L. Mancuso, N. Ferrari, J. Davison, Operating flexibility of power plants with carbon capture and storage (CCS), Energy Procedia 37 (2013) 2727–2737, https://doi.org/10.1016/j.egypro.2013.06.157.
[6] Gerhard K. Lausterer, Improved maneuverability of power plants for better grid stability and economic dispatch, IFAC Proc. 30 (17) (1997) 589–594, https://doi.org/10.1016/S1474-6670(17)46469-X.
[7] M. Huebel, C. Gierow, J.H. Prause, S. Meinke, E. Hassel, Simulation of ancillary services in thermal power plants in energy systems with high impact of renewable energy, (2017), doi: 10.1115/POWER-ICOPE2017-3258.
[8] Yongliang Zhao, Chaoyang Wang, Ming Liu, Daotong Chong, Junjie Yan, Improving operational flexibility by regulating extraction steam of high-pressure heaters on a 660 MW supercritical coal-fired power plant: a dynamic simulation, Appl. Energy 212 (2018) 1295–1309, https://doi.org/10.1016/j.apenergy.2018.01.017.
[9] T. Spitz, A. González Díaz, H. Chalmers, M. Lucquiaud, Operating flexibility of natural gas combined cycle power plant integrated with post-combustion capture, Int. J. Greenh. Gas Control. 88 (2019) 92–108, https://doi.org/10.1016/j.ijggc.2019.04.023.
[10] D.L. Oates, P. Versteeg, E. Hittinger, P. Jaramillo, Profitability of CCS with flue gas bypass and solvent storage, Int. J. Greenh. Gas Control. 27 (2014) 279–288, https://doi.org/10.1016/j.ijggc.2014.06.003.
[11] T. Van Peteghem, E. Delarue, Opportunities for applying solvent storage to power plants with post-combustion carbon capture, Int. J. Greenh. Gas Control. 21 (2014) 203–213, https://doi.org/10.1016/j.ijggc.2013.12.010.
[12] Dalia Patiño-Echeverri, David C. Hoppock, Reducing the energy penalty costs of postcombustion CCS systems with amine-storage, Environ. Sci. Technol. 46 (2) (2012) 1243–1252, https://doi.org/10.1021/es202164h.
[13] N. Ferrari, L. Mancuso, P. Cotone, Operating flexibility of power plants with CCS, Foster Wheel. Ital. (2012) 817. ieaghg.org/docs/General_Docs/Reports/2012-06 Reduced.pdf.
[14] Nicolas Perrin, Richard Dubettier, Frederick Lockwood, Jean-Pierre Tranier, Claire Bourhy-Weber, Paul Terrien, Oxycombustion for coal power plants: advantages, solutions and projects, Appl. Therm. Eng. 74 (2015) 75–82, https://doi.org/10.1016/j.applthermaleng.2014.03.074.
[15] D.P. Hanak, D. Powell, V. Manovic, Techno-economic analysis of oxy-combustion coal-fired power plant with cryogenic oxygen storage, Appl. Energy. 191 (2017) 193–203, https://doi.org/10.1016/j.apenergy.2017.01.049.

[16] M. Nimtz, H.J. Krautz, Flexible operation of CCS power plants to match variable renewable energies, Energy Procedia 40 (2013) 294–303, https://doi.org/10.1016/j.egypro.2013.08.034.
[17] B. Arias, An analysis of the operation of a flexible oxy-fired CFB power plant integrated with a thermal energy storage system, Int. J. Greenh. Gas Control. 45 (2016) 172–180, https://doi.org/10.1016/J.IJGGC.2015.12.007.
[18] S. Rezvani, D. McIlveen-Wright, Y. Huang, A. Dave, J.D. Mondol, N. Hewitt, Comparative analysis of energy storage options in connection with coal fired Integrated Gasification Combined Cycles for an optimised part load operation, Fuel 101 (2012) 154–160, https://doi.org/10.1016/j.fuel.2011.07.034.
[19] John Davison, Flexible CCS plants - a key to near-zero emission electricity systems, Energy Procedia 4 (2011) 2548–2555, https://doi.org/10.1016/j.egypro.2011.02.152.
[20] B. Arias, M.E. Diego, J.C. Abanades, M. Lorenzo, L. Diaz, D. Martínez, J. Alvarez, A. Sánchez-Biezma, Demonstration of steady state CO2 capture in a 1.7MWth calcium looping pilot, Int. J. Greenh. Gas Control. 18 (2013) 237–245, https://doi.org/10.1016/j.ijggc.2013.07.014.
[21] J. Kremer, A. Galloy, J. Ströhle, B. Epple, Continuous CO2 capture in a 1-MWth carbonate looping pilot plant, 36 (2013) 1518–1524, doi: 10.1002/ceat.201300084.
[22] J. Ströhle, M. Junk, J. Kremer, A. Galloy, B. Epple, Carbonate looping experiments in a 1 MWth pilot plant and model validation, Fuel 127 (2014) 13–22, https://doi.org/10.1016/j.fuel.2013.12.043.
[23] Jochen Ströhle, Jochen Hilz, Bernd Epple, Performance of the carbonator and calciner during long-term carbonate looping tests in a 1 MWth pilot plant, J. Environ. Chem. Eng. 8 (1) (2020) 103578, https://doi.org/10.1016/j.jece:2019.103578.
[24] Heiko Dieter, Craig Hawthorne, Mariusz Zieba, Günter Scheffknecht, Progress in calcium looping post combustion CO2 capture: successful pilot scale demonstration, Energy Procedia 37 (2013) 48–56, https://doi.org/10.1016/j.egypro.2013.05.084.
[25] Heiko Dieter, Ajay R. Bidwe, Glykeria Varela-Duelli, Alexander Charitos, Craig Hawthorne, Günter Scheffknecht, Development of the calcium looping CO2 capture technology from lab to pilot scale at IFK, University of Stuttgart, Fuel 127 (2014) 23–37, https://doi.org/10.1016/j.fuel.2014.01.063.
[26] M.E. Diego, B. Arias, A. Méndez, M. Lorenzo, L. Díaz, A. Sánchez-Biezma, J. C. Abanades, Experimental testing of a sorbent reactivation process in La Pereda 1.7 MWth calcium looping pilot plant, Int. J. Greenh. Gas Control. 50 (2016) 14–22, https://doi.org/10.1016/j.ijggc.2016.04.008.
[27] M.E. Diego, B. Arias, J.C. Abanades, Evolution of the CO2 carrying capacity of CaO particles in a large calcium looping pilot plant, Int. J. Greenh. Gas Control. 62 (2017) 69–75, https://doi.org/10.1016/j.ijggc.2017.04.005.
[28] M.E. Diego, B. Arias, J.C. Abanades, Investigation of the dynamic evolution of the CO2 carrying capacity of solids with time in La Pereda 1.7 MWth calcium looping pilot plant, Int. J. Greenh. Gas Control. 92 (2020) 102856, https://doi.org/10.1016/j.ijggc.2019.102856.
[29] M.E. Diego, B. Arias, Impact of load changes on the carbonator reactor of a 1.7 MWth calcium looping pilot plant, Fuel Process. Technol. (2020), https://doi.org/10.1016/j.fuproc.2019.106307.
[30] Y.A. Criado, B. Arias, J.C. Abanades, Calcium looping CO2 capture system for back-up power plants, Energy Environ. Sci. 10 (9) (2017) 1994–2004, https://doi.org/10.1039/C7EE01505D.
[31] Borja Arias, Yolanda A. Criado, J. Carlos Abanades, Thermal integration of a flexible calcium looping CO2 capture system in an existing back-up coal power plant, ACS Omega 5 (10) (2020) 4844–4852, https://doi.org/10.1021/acsomega.9b0355210.1021/acsomega.9b03552.s001.
[32] Dawid P. Hanak, Chechet Biliyok, Vasilije Manovic, Calcium looping with inherent energy storage for decarbonisation of coal-fired power plant, Energy Environ. Sci. 9 (3) (2016) 971–983, https://doi.org/10.1039/C5EE02950C.
[33] Marco Astolfi, Edoardo De Lena, Matteo C. Romano, Improved flexibility and economics of Calcium Looping power plants by thermochemical energy storage, Int. J. Greenh. Gas Control. 83 (2019) 140–155, https://doi.org/10.1016/j.ijggc.2019.01.023.
[34] GECOS, GS software, 2016. Available from: <www.gecos.polimi.it>.
[35] Matteo C. Romano, Modeling the carbonator of a Ca-looping process for CO2 capture from power plant flue gas, Chem. Eng. Sci. 69 (1) (2012) 257–269, https://doi.org/10.1016/j.ces.2011.10.041.
[36] M.M. Shah, Carbon dioxide (CO 2) compression and purification technology for oxy-fuel combustion, in: L.B.T.-O.-F.C. for P.G. and C.D. (CO2) C. Zheng (Ed.), Oxy-Fuel Combust. Power Gener. Carbon Dioxide Capture, Elsevier, 2011, pp. 228–255, doi: 10.1533/9780857090980.2.228.
[37] International Energy Agengy, Oxy Combustion Processes for CO 2 Capture from Power Plant, IEA Greenh. Gas R&D Program. (2005) 212. Available from: <https://ieaghg.org/docs/General_Docs/Reports/Report 2005-9 oxycombustion.pdf>.
[38] A. Błaszczuk, W. Nowak, S. Jagodzik, Bed-to-wall heat transfer in a supercritical circulating fluidised bed boiler, Chem. Process Eng. - Inz. Chem. i Proces. 35 (2014) 191–204, https://doi.org/10.2478/cpe-2014-0015.
[39] J. Hilz, M. Helbig, M. Haaf, A. Daikeler, J. Ströhle, B. Epple, Investigation of the fuel influence on the carbonate looping process in 1 MWth scale, Fuel Process. Technol. 169 (2018) 170–177, https://doi.org/10.1016/J.FUPROC.2017.09.016.
[40] Isabel Martínez, Gemma Grasa, Jarno Parkkinen, Tero Tynjälä, Timo Hyppänen, Ramón Murillo, Matteo C. Romano, Review and research needs of Ca-Looping systems modelling for post-combustion CO2 capture applications, Int. J. Greenh. Gas Control. 50 (2016) 271–304, https://doi.org/10.1016/j.ijggc.2016.04.002.
[41] D.P. Hanak, S. Michalski, V. Manovic, From post-combustion carbon capture to sorption-enhanced hydrogen production: a state-of-the-art review of carbonate looping process feasibility, Energy Convers. Manag. 177 (2018) 428–452, https://doi.org/10.1016/j.enconman.2018.09.058.
[42] Thermoflow Inc., Thermoflex v.27.0, 2018. Available from: <www.thermoflow.com>.
[43] S.J. Goidich, S. Wu, Z. Fan, A.C. Bose, Design aspects of the ultra-supercritical CFB boiler, in: 22nd Annu. Int. Pittsburgh Coal Conf. 2005, PCC 2005, 2005.
[44] Z. Fan, S. Goidich, A. Robertson, S. Wu, Ultra-supercritical pressure CFB boiler conceptual design study, 2006, doi: 10.2172/908300.
[45] Yolanda A. Criado, Borja Arias, J. Carlos Abanades, Effect of the carbonation temperature on the CO2 carrying capacity of CaO, Ind. Eng. Chem. Res. 57 (37) (2018) 12595–12599, https://doi.org/10.1021/acs.iecr.8b02111.
[46] Electric Power Research Institute (EPRI), Program on Technology Innovation: Integrated Generation Technology Options 2012, 2013. Available from: <https://www.epri.com/research/products/000000000001026656>.
[47] Zero emissions platform (ZEP), The Costs of CO2 Capture, Transport and Storage, (2011) 50. Available from: <http://www.zeroemissionsplatform.eu/library/publication/165-zep-cost-report-summary.html>.